Journal of Medicinal Chemistry Article

J. Med. Chem. **2011,** *54,* 877–889 **877**
DOI: 10.1021/jm101349u

Synthesis and Biological Evaluation of a New Series of 1,2,4-Triazolo[1,5-*a*]-1,3,5-triazines as Human A_{2A} Adenosine Receptor Antagonists with Improved Water Solubility

Stephanie Federico,[#] Silvia Paoletta,[†] Siew Lee Cheong,[§] Giorgia Pastorin,[§] Barbara Cacciari,[‡] Stefano Stragliotto,[†] Karl Norbert Klotz,[∥] Jeffrey Siegel,[⊥] Zhan-Guo Gao,[⊥] Kenneth A. Jacobson,[⊥] Stefano Moro,*[,†] and Giampiero Spalluto*[,#]

[#]*Dipartimento di Scienze Farmaceutiche, Università di Trieste, Piazzale Europa 1, I-34127 Trieste, Italy,* [†]*Molecular Modeling Section (MMS), Dipartimento di Scienze Farmaceutiche, Università di Padova, via Marzolo 5, I-35131 Padova, Italy,* [§]*Department of Pharmacy, National University of Singapore, 3 Science Drive 2, Singapore 117543,* [‡]*Dipartimento di Scienze Farmaceutiche, Università degli Studi di Ferrara, via Fossato di Mortara 17-19, I-44100 Ferrara, Italy,* [∥]*Institut für Pharmakologie, Universität of Würzburg, D-97078 Würzburg, Germany, and* [⊥]*Molecular Recognition Section (MRS), Laboratory of Bioorganic Chemistry, National Institute of Diabetes and Digestive and Kidney Diseases, National Institutes of Health, Bethesda, Maryland, United States*

Received October 18, 2010

The structure−activity relationship (SAR) of 1,2,4-triazolo[1,5-*a*]-1,3,5-triazine derivatives related to ZM241385 as antagonists of the A_{2A} adenosine receptor (AR) was explored through the synthesis of analogues substituted at the 5 position. The A_{2A} AR X-ray structure was used to propose a structural basis for the activity and selectivity of the analogues and to direct the synthetic design strategy to provide access to solvent-exposed regions. Thus, we have identified a point of substitution for the attachment of solubilizing groups to enhance both aqueous solubility and physicochemical properties, maintaining potent interactions with the A_{2A} AR and, in some cases, receptor subtype selectivity. Among the most potent and selective novel compounds were a long-chain ether-containing amine congener **20** (K_i 11.5 nM) and its urethane-protected derivative **14** (K_i 17.8 nM). Compounds **20** and **31** (K_i 11.5 and 16.9 nM, respectively) were readily water-soluble up to 10 mM. The analogues were docked in the crystallographic structure of the hA_{2A} AR and in a homology model of the hA_3 AR, and the *per residue* electrostatic and hydrophobic contributions to the binding were assessed and stabilizing factors were proposed.

Adenosine receptors (ARs)[a] are members of the family of G protein-coupled receptors (GPCRs), and are classified as four subtypes, the A_1AR, A_{2A}AR, A_{2B}AR, and A_3AR,[1] which exert their physiological functions through the activation or inhibition of various second messenger systems. In particular, the modulation of adenylyl cyclase activity could be considered to be the principal signal mediated by these receptor subtypes.[2,3]

Activation or blockade of ARs is responsible for a wide range of effects in numerous organ systems raising the possibility that the regulation of ARs has potential therapeutic applications. The cardioprotective[2,3] and neuroprotective[4,5] effects associated with AR activation have been clearly demonstrated during periods of cardiac and cerebral ischemia, respectively. In addition, the use of antagonists of distinct AR subtypes could be useful in the treatment of asthma[6,7] or certain neurological diseases such as Parkinson's disease.[7,8] The pathophysiological roles of ARs and their clinical potential have been recently reviewed exhaustively.[7−12]

In recent years, an intensive effort performed by several groups led to the synthesis of a large variety of AR agonists and antagonists for the pharmacological characterization of this family of G protein-coupled receptors.[13] Among classes of AR antagonists, diverse heterocyclic derivatives have been proposed and found to display a range of affinities and selectivities. In particular, our groups have extensively investigated the pyrazolotriazolopyrimidine nucleus for AR antagonists. Optimization of the substituents at the N5, N7, N8, and C2 positions led to potent and selective A_{2A} and A_3 AR antagonists, for example, compounds **1** and **2** (Chart 1).[14−22]

Nevertheless, most of these heterocyclic derivatives, including other tricyclic structures, suffered from limited aqueous solubility and, most importantly, difficulties in their synthetic preparation.

Taking into account these problems, in recent years the synthesis of more simplified heterocyclic derivatives has been explored. In particular, bicyclic systems such as adenine,[23] triazolopyrazine,[24−26] and triazolotriazine[27−29] could be considered some of the most promising targets. The triazolotriazine nucleus was one of the most appealing bicyclic cores, which led previously to the discovery of 4-[2-[7-amino-2-(2-furyl)-1,2,4-triazolo[1,5-*a*][1,3,5]triazin-5-yl-amino]ethylphenol (ZM241385, **3**), that is, one of the most potent and selective A_{2A} AR antagonists known.[30,31] This compound also binds with good affinity to the human (h) A_{2B} AR (28 nM), and its tritiated form is a

*To whom correspondence should be addressed. Tel.: +39 040 5583726 (G.S.), +39 049 8275704 (S.M.). Fax: +39 040 52572 (G.S.), +39 049 8275366 (S.M.). E-mail: spalluto@units.it (G.S.); stefano.moro@unipd.it (S.M.).

[a] Abbreviations: AR, adenosine receptor; CHO, Chinese hamster ovary; DMSO, dimethylsulfoxide; DPCPX, 8-cyclopentyl-1,3-dipropylxanthine; EDTA, ethylenediaminetetraacetic acid; GPCR, G protein-coupled receptor; HEK, human embryonic kidney; I-AB-MECA, 1-[6-[[(4-amino-3-iodophenyl)methyl]amino]-9H-purin-9-yl]-1-deoxy-*N*-methyl-*β*-D-ribofuranuronamide; NECA, 5′-*N*-ethylcarboxamidoadenosine; TLC, thin layer chromatography; ZM241385, 4-[2-[7-amino-2-(2-furyl)-1,2,4-triazolo[1,5-*a*]-[1,3,5]triazin-5-yl-amino]ethylphenol, SAR, structure−activity relationship; TM, transmembrane; rmsd, root-mean-square deviation; EL2, second extracellular loop.

Published on Web 01/07/2011

Chart 1. Pyrazolotriazolopyrimidines as A_{2A} and A_3 AR Antagonists

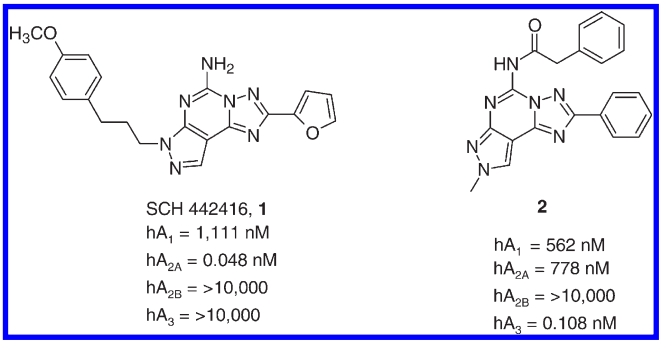

Chart 2. Triazolotriazines as A_{2A} AR Antagonists

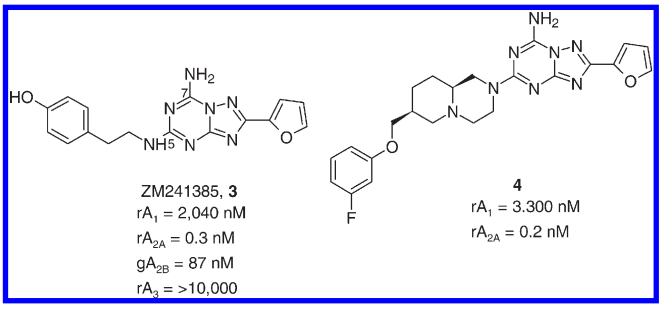

useful radioligand for this receptor subtype.[32] Recently, an intensive study of the structure activity relationship (SAR) of the triazolotriazine nucleus was reported, and compound **4** proved to be one of the most potent and selective for the A_{2A} AR as compared with the A_1 AR. Nevertheless, the lack of binding data at the A_{2B} and A_3 ARs prevented a comparison with other fully characterized derivatives (Chart 2).[27]

Very recently, our group performed a study on this nucleus trying to optimize substitution at the C5 and N7 positions with the aim of improving affinity and selectivity versus the hA_{2B} and hA_3 AR subtypes. In particular, inclusion at the N7 position of arylcarbamoyl (for A_3) or arylacetyl (for A_{2B}) moieties, which gave good results in the pyrazolotriazolopyrimidine family, has been investigated.[33] Unfortunately, none of these substitutions led to the desired selectivity; in fact introduction of bulky substituents at the N7 position (e.g., compound **5**) significantly increased the potency at the hA_3 AR with respect to reference compound **3** leading to low selectivity versus the A_1 AR. In contrast, a free amino group at the 7 position (compound **6**) provided intermediate potency at the A_{2B} AR, but the potency at the A_{2A} AR still predominated (Chart 3).[33]

Considering these experimental observations, we decided to further investigate the potential of this nucleus, in particular, by exploring the C5 position through the introduction of substituted amino or diamino functions (Chart 4), with the aim to modulate the activity at the A_{2A} and A_{2B} ARs and importantly to improve the water solubility, which would otherwise limit their use as pharmacological tools. In contrast, this new class of derivatives mainly contained a free amino group at the 7 position, but small substituents were introduced in a few compounds with the aim of increasing the interaction in the receptor binding pocket.

The analogues synthesized have been evaluated for potency at all four hARs, and the results obtained were interpreted with the help of computational methodologies.

Chart 3. Examples of Triazolotriazines as Nonselective A_{2B} and A_3 AR Antagonists

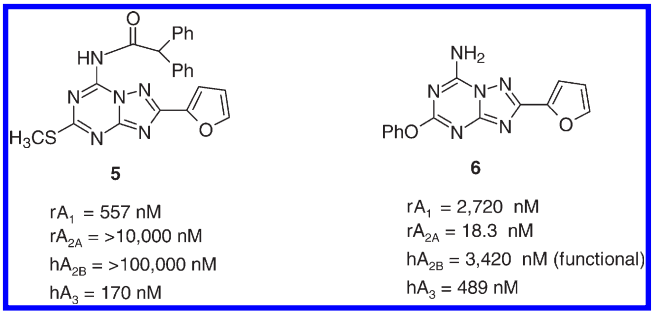

Chart 4. Designed and Synthesized Compounds **7**−**43**

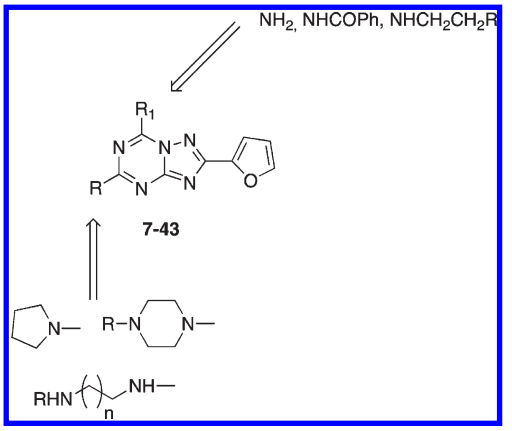

Chemistry

The designed compounds (**7**−**43**) were synthesized as summarized in Schemes 1−3. Reacting the well-known key intermediate **44**[34] with pyrrolidine (**51**) or the appropriate mono-*tert*-butyloxy-protected diamine (**45**−**50**), prepared as previously reported,[35] in ethanol solution in a sealed tube at 120 °C, the desired 5-substituted triazolotriazine derivatives (**7**, **10**−**14**) were obtained. Treatment of these compounds (**7**, **10**−**14**) with 10% trifluoroacetic acid in CH_2Cl_2 at room temperature led to the corresponding amino derivatives (**9**, **20**, **30**−**33**) as trifluoroacetate salts (Scheme 1). Alternately, by reacting **44** with an excess of mono-Boc-ethylendiamine (**47**) in a sealed tube at 180 °C the 5,7-disubstituted derivative (**37**) was obtained. After *N*-Boc deprotection in acidic conditions, the *bis*-trifluoroacetate salt **38** was obtained (Scheme 1).

By treatment of derivative **9** with the appropriate benzyl halide or acyl chloride in dry dioxane in the presence of Et_3N at room temperature, the corresponding *N*-benzyl (**15**−**19**) or *N*-acyl (**21**−**29**, **34**−**36**) derivatives were obtained (Scheme 2).

Disubstituted derivatives at the 5 and 7 positions (**39**−**43**) were prepared starting from **44** as depicted in Scheme 3. Treating **44** with ethanolic ammonia in a sealed tube at 120 °C afforded derivative **41**. Otherwise, acylation at the 7 position with benzoyl chloride in standard conditions led to compound **39**, which after treatment in a sealed tube at 120 °C with ethanolic ammonia gave compound **43** (Scheme 3).

Instead, treatment of **44** with 2 N KOH in ethanol at reflux led to the 5-hydroxy derivative **40**, which after treatment with benzoyl chloride in the presence of Et_3N afforded the desired product **42**.

Scheme 1[a]

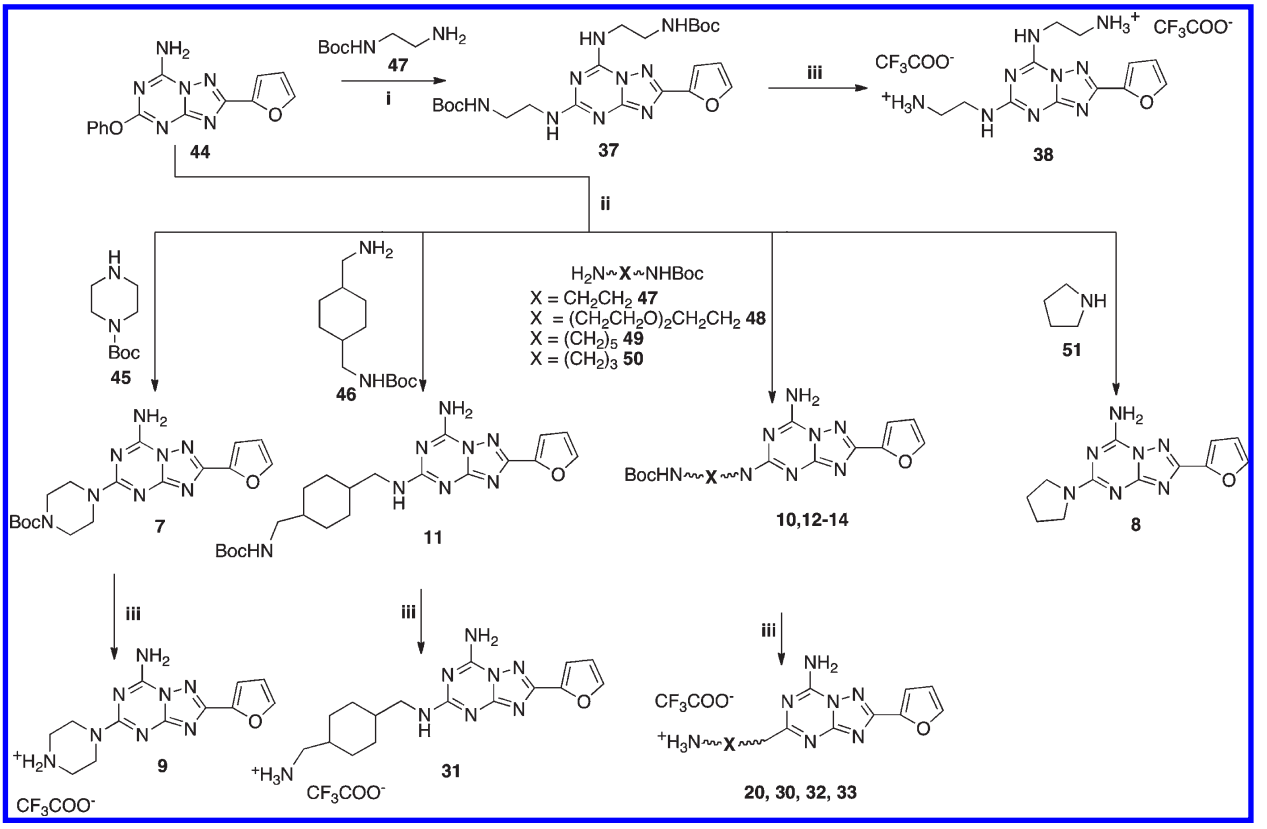

[a] Reagents: i: EtOH, sealed tube, amine excess, 180 °C; ii: EtOH, sealed tube 120 °C; iii: CF_3COOH, CH_2Cl_2, rt.

Scheme 2[a]

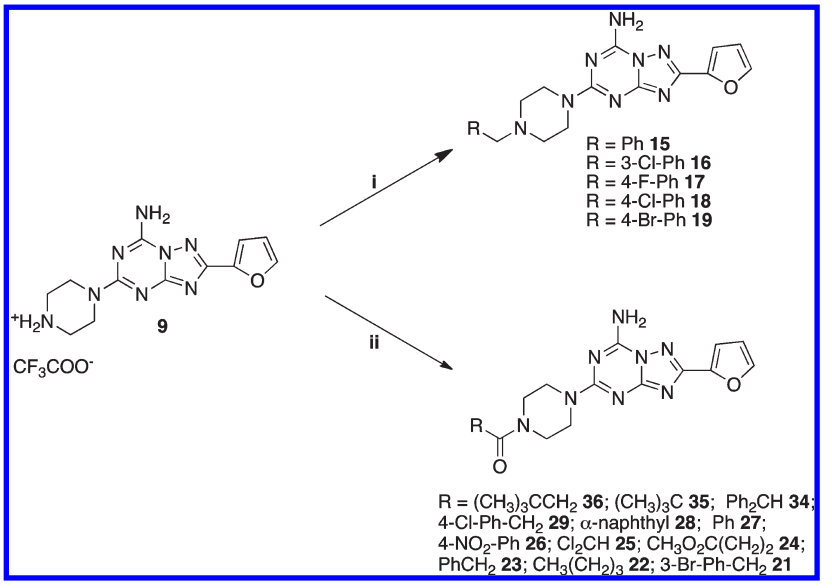

[a] Reagents: i: RCH_2Br, Et_3N, dioxane, rt; ii: RCOCl, Et_3N, dioxane, rt.

Molecular Modeling

To better define the SAR profile of the AR antagonists reported herein, a molecular modeling study was performed. The recently published X-ray crystallographic structure of the hA_{2A} AR, in complex with the high affinity antagonist ZM241385 (PDB code: 3EML),[36] provides useful three-dimensional structural information for performing molecular docking studies of A_{2A} AR antagonists. Therefore, all the synthesized compounds were docked to the binding cavity of the A_{2A} AR crystal structure, in order to evaluate their binding mode at this receptor subtype. Moreover, to explain the A_{2A}/A_3 selectivity profile, docking simulations were also performed at the hA_3 AR binding site. Since no crystallographic information is available for the A_3 subtype, a previously proposed homology model of the hA_3 AR based on the crystal structure of the hA_{2A} AR was used to perform the docking studies.[37,38]

Scheme 3[a]

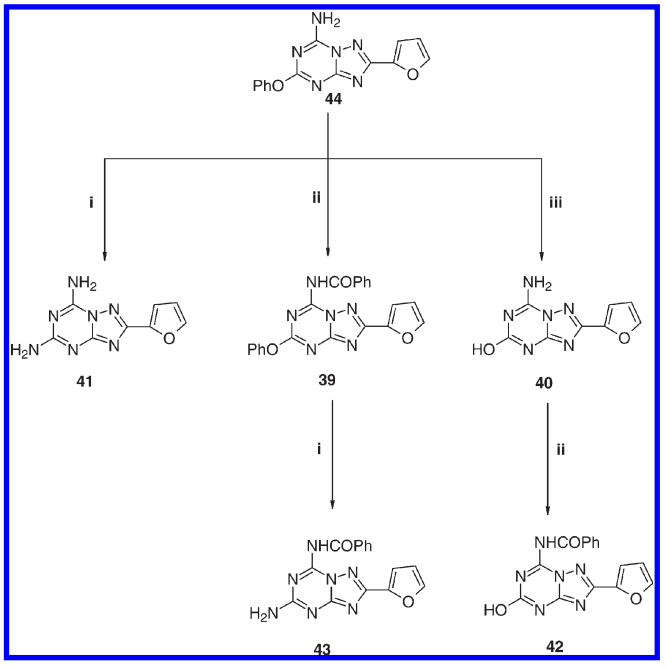

[a] Reagents: i: NH_3, EtOH, sealed tube, 120 °C; ii: PhCOCl, Et_3N, dioxane reflux; iii: KOH, EtOH reflux.

In the initial process of selecting a reliable docking protocol to be employed in docking studies of the new derivatives, we have evaluated the ability of different docking software programs to reproduce the crystallographic pose of ZM241385 inside the binding cavity of hA_{2A} AR. As reported in the Experimental Section, among the four different programs used to calibrate our docking protocol, the Gold program was finally chosen because it showed the best performance with respect to the calculated rmsd values relative to the crystallographic pose of ZM241385.[37,39]

Consequently, on the basis of the selected docking protocol, we performed docking simulations to identify the hypothetical binding mode of the new 1,2,4-triazolo[1,5-*a*]-1,3,5-triazines inside the crystallographic structure of hA_{2A} AR and the hA_3 AR model. All the newly synthesized compounds were docked into the orthosteric transmembrane (TM) binding cavities of both ARs. Additionally, in order to analyze the possible ligand−receptor recognition mechanism in a more quantitative manner, we calculated the individual electrostatic and hydrophobic contributions to the interaction energy of each receptor residue involved in the binding with ligands. Using the calculated electrostatic and hydrophobic contributions values, color maps of electrostatic and hydrophobic interactions *per residue* were constructed.

Results and Discussion

Table 1 reports the receptor binding affinities of the synthesized compounds (**7**−**43**). The binding properties were determined at the hA_1, hA_{2A}, and hA_3 ARs expressed in human embryonic kidney (HEK)-293 cells using as radioligands: [^{3}H]8-cyclopentyl-1,3-dipropylxanthine ([^{3}H]DPCPX, A_1);[40] [^{3}H]-(4-(2-[7-amino-2-(2-furyl)[1,2,4]triazolo[2,3-a][1,3,5]triazin-5-yl-amino]ethyl)-4-iodo-phenol, ([^{3}H]ZM241385, A_{2A});[41] or in Chinese hamster ovary (CHO) cells using [^{125}I]N^6-(4-amino-3-iodobenzyl)-5′-*N*-methylcarbamoyladenosine ([^{125}I]I-AB-MECA, A_3).[42] Because of the lack of a suitable hA_{2B} AR radioligand, the activity of antagonists was determined in adenylyl cyclase experiments in CHO cells expressing the hA_{2B} AR.[43,44]

As clearly indicated in Table 1, all the analogues were in general nearly inactive at the hA_3 AR independent of the substitution at the 5 and 7 positions, with the exception of compounds **10** and **29** having affinity in the range of 1 μM. A similar behavior, in contrast to expectations, could be observed at the hA_{2B} AR; in fact all the analogues were inactive or poorly active (e.g., compounds **11**, **31**, **41**, **43**) in the functional assay. Nevertheless, the binding profile of this class of compounds at the hA_{2A} AR demonstrated affinity in the nanomolar range and with different degrees of selectivity versus the hA_1 AR subtype.

Insertion at the C5 position of amino or mono-Boc-diamino (compounds **7**, **8**, **10**−**14**) functionality led to compounds with good affinity at the hA_{2A} AR (range 18−70 nM) with variable selectivity versus the A_1 AR. In particular, the presence of a pyrrolidine (**8**) at the 5 position favored affinity at the A_{2A} AR (59.1 nM) but poor selectivity (33-fold) versus the A_1 subtype, while introduction of Boc-piperidine (**7**) or Boc-ethylendiamine (**10**) seem to improve both affinity and selectivity at the A_{2A} AR (e.g compound **7**, hA_{2A} = 21 nM, A_1/A_{2A} = 257). Interestingly, elongation of the diamino chain at the C5 position to 3 or 5 carbon atoms (compounds **12**, **13**) led to derivatives which still retained good affinity at the hA_{2A} AR but less selectivity versus the A_1 subtype (e.g., compound **13** hA_{2A} = 44.7 nM, A_1/A_{2A} = 21.5), while longer chains such as a Boc-triethylenoxydiamino moiety (**14**) gave good results both in terms of affinity and selectivity (hA_{2A} = 17.8 nM, A_1/A_{2A} = 89).

Trifluoroacetate salt derivatives (**9**, **30**−**33**) were in general less potent than the corresponding Boc derivatives (e.g., compound **7**, hA_{2A} = 21 nM, A_1/A_{2A} = 257 versus compound **9**, hA_{2A} = 153 nM, A_1/A_{2A} = 65). An exception occurred when long or bulky chains were present at the C5 position. In fact, compounds **20** and **31** were more potent at the hA_{2A} AR than the corresponding Boc derivatives (e.g., compound **31**, hA_{2A} = 16.9 nM, A_1/A_{2A} = 79; compound **11**: hA_{2A} = 69.7 nM, A_1/A_{2A} = 56), but most importantly both compounds were readily water-soluble up to 10 mM. In particular, compound **20**, which displayed an affinity at the hA_{2A} AR of 11.5 nM and good selectivity versus A_1, was the most potent compound of this series. Despite this relevant improvement of the water solubility other pharmacokinetics properties, such as cell permeation or metabolic stability, are collecting in our laboratories before setting up any further in vivo testing.

Interestingly, double substitution with diamino functions at the C5 and N7 positions led to completely inactive compounds at all four AR subtypes, both as protected (**37**) or deprotected (**38**) forms.

An altered binding profile was observed for the piperazine derivatives alkylated or acylated at the piperazine secondary amine. In particular, in the *N*-benzyl series (**15**−**19**) good affinity at the hA_{2A} AR was retained, but also an increased affinity at the hA_1 was observed with a consequent reduction of selectivity, independently of the type of substitution on the phenyl ring.

A more complex profile was present when an acyl group was present on the piperazine secondary amine. In particular, when a benzoyl group was introduced on the piperazine nitrogen (**26**, **27**) a significant reduction of affinity at the hA_{2A} AR (range 212−348 nM) was observed with a subsequent reduction of selectivity (35−48 fold). If the phenyl ring was replaced with a more bulky substituent such as a naphthyl

Table 1. Structures and Binding Profile of Synthesized Compounds **7**−**43**

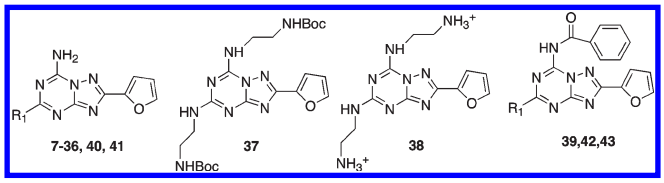

Compd	R^1	hA_1 % displ 10μM (or K_i, nM)[a]	hA_{2A} (K_i, nM)[b]	hA_{2B} IC_{50} (nM)[c]	hA_3 % displ 10μM (or K_i, nM)[d]	hA_1/hA_{2A}	hA_3/hA_{2A}
7		5400 ± 500	21 ± 4.5	>10,000	56.6 ± 1.3%	257	~400
8		1940 ± 70	59.1 ± 13.7	>30,000	75.0 ± 4.7%	33	e
9		28.6 ± 6.0%	153 ± 32	>30,000	29.9 ± 0.4%	>65	>65
37	-	7.4 ± 4.5%	4360 ± 1670	>100,000	8490 ± 4810	>2	1.9
10	$NH\text{-}(CH_2)_2NHBoc$	3730 ± 740	40.9 ± 5.7	>10,000	1490 ± 480	91	36
11	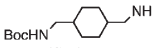	3,890 ± 560	69.7 ± 12.7	7140 ± 2960	75.5 ± 0.3%	56	e
12	$NH\text{-}(CH_2)_3NHBoc$	344 ± 16	38.6 ± 11.5	20,600 ± 1100	77.3 ± 0.3%	9	e
13	$NH\text{-}(CH_2)_5NHBoc$	963 ± 139	44.7 ± 9.9	>10,000	68.6 ± 0.9%	21.5	e
14	$NH\text{-}(CH_2CH_2O)_2\text{-}(CH_2)_2NHBoc$	1580 ± 100	17.8 ± 6.7	>10,000	74.0 ± 0.8%	89	e
15		978 ± 146	20.6 ± 14.5	>30,000	71.9 ± 0.7%	47.5	e
16		1510 ± 500	51.8 ± 23.0	>30,000	52.7 ± 1.2%	29	~200
17		655 ± 100	52.3 ± 32.3	>10,000	71.3 ± 1.9%	12.5	e
18		220 ± 88	102 ± 108	>30,000	66.8 ± 6.0%	2.1	e
19		86.7 ± 22.6	27.3 ± 18.0	>10,000	49.8 ± 0.8%	3.2	~300
20	$NH\text{-}(CH_2CH_2O)_2\text{-}(CH_2)_2NH_3^+$	769 ± 308	11.5 ± 2.2	>10,000	59.2 ± 2.6%	67	e
21		1,010 ± 150	86.2 ± 41.4	>30,000	3100 ± 1100	11.7	36
22		10.8 ± 5.3%	124 ± 50	>100,000	56.2 ± 8.1%	>81	e
23		3510 ± 220	94.8 ± 40.7	>100,000	64.5 ± 1.8%	37	e
24		19.4 ± 2.5%	66.2 ± 10.4	>100,000	37.2 ± 6.6%	>150	>150
25		34.6 ± 1.5%	282 ± 164	>100,000	33.6 ± 0.7%	>36	>36
26		35.5 ± 7.4%	212 ± 49	>100,000	50.9 ± 6.9%	>47	~40
27		27.7 ± 3.3%	348 ± 76	>100,000	22.6 ± 1.7%	>29	>29
28		4.9 ± 0.8%	7680 ± 2190	>100,000	31.1 ± 8.4%	>1.3	>1.3
29		991 ± 226	39.1 ± 13.9	>100,000	1260 ± 490	25	32
38	-	10.7 ± 1.5%	38,200 ±14,600	>100,000	17.7 ± 3.6%	0.3	e
30	$NH\text{-}(CH_2)_2NH_3^+$	35.8 ± 4.9%	567 ± 43	>100,000	30.8 ± 3.7%	>18	>18
31	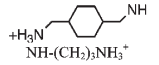	1350 ± 70	16.9 ± 2.3	10,700 ± 3,700	72.8 ± 0.4%	79	e
32	$NH\text{-}(CH_2)_3NH_3^+$	44.3 ± 1.6%	270 ± 9	>30,000	40.5 ± 0.2%	>37	>37
33	$NH\text{-}(CH_2)_5NH_3^+$	2,950 ± 260	90.1 ± 15.9	>10,000	49.9 ± 3.5%	33	~100
34		7470 ± 6820	92.9 ± 24.7	>100,000	40.6 ± 22.2%	80	~100
35		38.7 ± 4.8%	58.4 ± 18.9	>100,000	32.3 ± 3.37%	>170	>170
36		53.1 ± 4.7%	11.1 ± 6.3	>100,000	41.9 ± 8.3%	~900	>900
39	OPh	26.2 ± 5.5%	1000 ± 110	>10,000	32.3 ± 9.7%	>10	>10
40	OH	3110 ± 970	201 ± 61	>10,000	43.9 ± 6.0%	15.5	~50
41	NH_2	1410 ± 80	160 ± 42	11,100 ± 3,900	36.4 ± 0.2%	9	>60
42	OH	34.4 ± 9.2%	1750 ± 390	>100,000	75.9 ± 1.2%	>6	e
43	NH_2	1800 ± 150	44.1 ± 13.6	7060 ± 2935	67.2 ± 3.3%	40	e

[a] Displacement of specific [^{3}H]DPCPX binding at the hA_1 AR expressed in HEK-293 cells. [b] Displacement of specific [^{3}H]ZM241385 binding at hA_{2A} AR expressed in HEK-293 cells. Data are expressed as K_i ± SEM in nM (n = 3−6). [c] Measurement of adenylyl cyclase activity in CHO cells stably transfected with recombinant hA_{2B} AR, expressed as IC_{50} (nM). [d] Displacement of specific [^{125}I]I-AB-MECA binding at hA_3 receptors expressed in CHO cells. Data are expressed as K_i ± SEM in nM (n = 3−6). [e] Selectivity not determined or estimated.

nucleus (compound **28**), a complete loss of affinity at all four hARs was observed.

If the aroyl group was replaced with an aryl acetyl moiety, significant differences could be observed in the binding profile. In particular, introduction of a phenylacetyl (**23**) or a 4-substituted-phenylacetyl group (**21**, **29**) at the piperazine secondary amine led to compounds that still retained good affinity at the hA_{2A} AR in the range of 40−95 nM with poor selectivity versus A_1 (12−37 fold). In contrast, introduction of a bulky substituent such as a diphenylacetyl moiety (**34**) provided a compound with a quite good affinity at the hA_{2A} AR (hA_{2A} = 93 nM). Importantly, the selectivity versus the hA_1 subtype (A_1/A_{2A} = 80) was high, which was exactly the opposite observed for the nearly inactive bulky aroyl derivative **28**.

A quite different profile could be observed when the piperazine secondary amine was acylated with alkyl groups. In particular, introduction of a small group (**25**) or unbranched chains (**22**, **24**) led to compounds which proved to be quite potent (range 66−280 nM) at the hA_{2A} AR. Branched chains such as *tert*-butylcarbonyl (**35**) and 3,3-dimethylbutanoyl (**35**) increased the affinity at the hA_{2A} AR and significantly increased selectivity versus the hA_1 subtype. In particular, derivative **36** showed high affinity at the hA_{2A} AR (11.1 nM) and 900-fold selectivity versus the hA_1 subtype.

The derivatives substituted both at the C5 and N7 positions with small groups (**39**−**43**) showed in general weak affinity at the hA_{2A} AR and low levels of selectivity. Moreover, the diamino compound **41** and the corresponding 5-hydroxy derivative **40** showed hA_{2A} affinity in the high nanomolar range (160−200 nM), but the levels of selectivity versus the hA_1 AR were very low, ranging from 2 to 12. When a benzoyl group was present at the N7 position, the presence at the C5 position of a hydroxy (**42**) or phenoxy (**39**) moiety greatly reduced activity at the four ARs, with affinity at the hA_{2A} subtype in the micromolar range. In contrast, when an amino group was present at the C5 position, affinity at the hA_{2A} AR (hA_{2A} = 44.1 nM) was recovered with good levels of selectivity versus other receptor subtypes.

In order to rationalize the observed binding data, a molecular modeling investigation was performed for all the newly synthesized analogues using both the crystallographic structure of hA_{2A} AR and the hA_3 AR model. The analysis was extended to docking simulations and *per residue* electrostatic and hydrophobic contributions maps.

The first important consideration is that almost all the selected poses at the hA_{2A} AR of these new analogues showed some common features, as highlighted by the calculated electrostatic and hydrophobic contributions to the interaction energy collected in Figure 1. In particular, all ligands made contacts mainly with residues belonging to TM2, TM3, TM6, TM7, and EL2.

The *per residue* electrostatic interaction energy map (Figure 1A) showed two bands with negative energy (colored in green) corresponding to Glu169 in EL2 and Asn253 in TM6, indicating that these two residues were responsible for the main electrostatic interactions with all the tested analogues, with a few exceptions. On the other hand, the map of the *per residue* hydrophobic interaction score (Figure 1B) highlighted several residues involved in hydrophobic contacts with ligands, including Leu85 in TM3, Phe168 in EL2, Trp246, Leu249, His250 in TM6 and Tyr271, Ile274 in TM7. Therefore, the analysis of these maps gave important preliminary data concerning similarity and differences in the binding modes at the hA_{2A} AR of these new

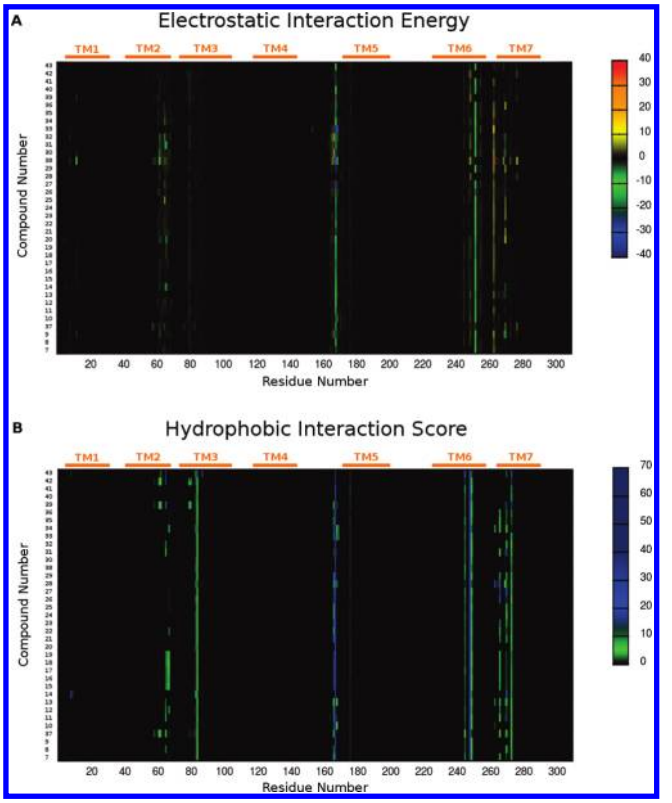

Figure 1. (A) *Per residue* electrostatic interaction energy map and (B) *per residue* hydrophobic interaction score map. The maps are calculated for a selected pose of each compound (**7**−**43**) inside the hA_{2A} AR binding site. Electrostatic energy values are expressed in kcal/mol, while hydrophobic scores are expressed in arbitrary hydrophobic units.

compounds; this information was then confirmed by a detailed investigation of the docking poses as reported below.

Docking of 7-Amino Derivatives (Compounds 7−36, 40, and 41). From the docking simulation analysis, all the new derivatives with free amino group at the 7 position, with the exception of compound **28**, were seen to share a similar binding pose in the TM region of the hA_{2A} AR. For these compounds, ligand-recognition occurred in the upper region of the TM bundle, and the triazolotriazine nucleus was surrounded by TMs 3, 5, 6, 7 with the 2-furyl ring located deep in the binding cavity.

Considering Figure 2, it is evident that the binding poses of these ligands were very similar to the crystallographic pose of ZM241385 bound to the hA_{2A} AR.[36] In fact, the triazolotriazine cores were completely superposable, while the only slight difference was in the orientation of the substituents at the 5-position. Moreover, all the crucial interactions established by ZM241385 with amino acid residues of the hA_{2A} AR binding site were also found for all these new 7-amino derivatives.

The analysis in Figure 3 (panel A) showing the hypothetical binding pose of compound **36** (K_i hA_{2A} = 11.1 nM) at the hA_{2A} AR helps to clarify this point. It appeared that the bicyclic triazolotriazine core was anchored within the binding cleft through an aromatic stacking interaction with Phe168 (EL2) and a H-bonding interaction with Asn253 (6.55). Moreover, the exocyclic amino group at the 7-position of the bicyclic core interacted with two polar residues, Asn253 (6.55) and Glu169 (EL2), forming two H-bonds. Interestingly, the important role in ligand binding of these

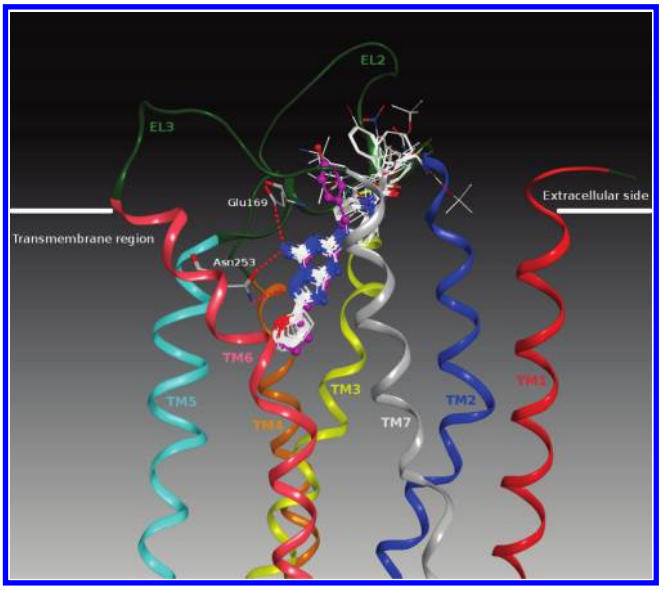

Figure 2. Structure superimposition of the crystallographic pose of ZM241385 (in magenta) and of the docking poses of all the 7-amino derivatives (in white) inside the hA_{2A} AR binding site. Side chains of some amino acids important for ligand recognition and H-bonding interactions are highlighted. Hydrogen atoms are not displayed.

two residues was previously revealed by site-directed mutagenesis studies.[45,46] The 4-(3,3-dimethylbutanoyl)-piperazinyl chain of the ligand was directed toward the more solvent-exposed extracellular region (EL2 and EL3) and interacted, through a H-bond, with Tyr271 (7.36). However, the furan ring was located deep within the ligand binding cavity and formed hydrophobic interactions with the highly conserved Trp246 (6.48), an important residue in receptor activation. Finally, compound **36** also formed hydrophobic interactions with many residues of the binding site including Val84 (3.32), Leu85 (3.33), Met177 (5.38), Leu249 (6.51), and Ile274 (7.39).

Analyzing the electrostatic contribution *per residue* to the whole interaction energy for the compound **36**−hA_{2A} AR complex (Figure 3C), the three main stabilizing factors were found to be related to Glu169 (EL2), Asn253 (6.55), and Tyr271 (7.36), due to the H-bonding interactions with the ligand above-described, whereas, as shown in Figure 3 (panel E), the hydrophobic interaction scores pattern showed two strong stabilizing contributions corresponding to the interactions of the bicyclic core with Phe168 (EL2) and Leu249 (6.51).

Therefore, as exemplified by the binding pose of compound **36**, all the newly synthesized 7-amino derivatives strongly interacted with the hA_{2A} AR in a manner similar to the crystallographic pose of ZM241385.[36] Moreover, these compounds, thanks to their different substituents at the 5 position, could variously interact with residues of the upper region of the receptor binding cavity, particularly in EL2 and EL3. Considering that the substituents at the 5 position were exposed to the highly plastic EL region and to solvent, it was difficult to define a clear SAR at the 5 position for this series.

On the other hand, the docking pose of compound **36** at the hA_3 AR was located in the same region of the TM bundle as at the hA_{2A} AR, but the orientation of the ligand was different (Figure 3B). In this case, the ligand formed only two H-bonds with Asn250 (6.55) and lost the aromatic interaction with Phe168 (EL2). The patterns of electrostatic and hydrophobic contribution to the energy of hA_3 AR-ligand complexes (Figure 3D,F) showed weaker *per residue* contributions compared to the ones at the hA_{2A} AR. Moreover, the residues present at the binding pocket entrance in the two AR subtypes possess very different features, which could affect both the orientation of the ligand while approaching the binding pocket and its accommodation into the final TM binding cleft, as already proposed for other compounds.[37] Therefore, both the lack of very strong interactions with the residues of the hA_3 AR and the differences at the binding site entrance are consistent with a lack of hA_3 affinity observed for the 7-amino derivative.

Among the 7-amino derivatives, only compound **28** (K_i hA_{2A} = 7680 nM) showed a different docking pose at the hA_{2A} AR (see Supporting Information). This ligand, probably due to the hindrance of the bulky and rigid α-naphthyl group, was not able to occupy the same position as the other 7-amino derivatives and consequently lost important H-bonding interactions with two critical residues of the hA_{2A} AR binding site, such as Glu169 (EL2) and Asn253 (6.55). In fact, in this docking pose the ligand formed only one H-bond with Tyr271 (7.36). This finding explained why compound **28** showed lower hA_{2A} AR affinity compared to the other 7-amino derivatives.

Docking of 7-(Alkyl/acyl)amino Derivatives (Compounds 37−39, 42 and 43). With the exception of compound **43**, all the 7-(alkyl/acyl)amino derivatives showed low affinity for the hA_{2A} AR (micromolar range). Docking studies revealed that compounds **37**−**39** and **42** possessed a different binding mode at the hA_{2A} AR compared to the 7-amino derivatives (see Supporting Information). In fact, the presence of an (alkyl/acyl)amino group at the 7 position prevented these compounds from forming a H-bonding network with Asn253 (6.55) and Glu169 (EL2), already seen to be critical for the binding of ZM241385 at this receptor subtype. This fact led these compounds to assume a different orientation inside the binding cavity of the receptor, although ligand-recognition occurred in the same upper region of the TM bundle, and the triazolotriazine nucleus was surrounded by TMs 3, 5, 6, 7 with the 2-furyl ring directed toward the inner part of the binding cavity. Therefore, their binding mode showed only a weak H-bond with Glu169 (EL2) and a stacking interaction with Phe168 (EL2). These findings were in agreement with the experimental data showing micromolar K_i values for these compounds.

In contrast to the 5 position derivatives described above, compound **43** (K_i hA_{2A} = 44.1 nM), due to the presence of a free amino group at C5, showed a characteristic mode of binding at the hA_{2A} AR (see Supporting Information). The triazolotriazine nucleus was oriented parallel to the membrane plane, and the 2-furyl ring was directed toward TM2, while the substituent at the 7 position was located in the inner part of the binding cavity. Compound **43** formed three H-bonding interactions, two with Asn253 (6.55) and one with Glu169 (EL2), and a $\pi-\pi$ stacking interaction with Phe168 (EL2). Therefore, the presence of a H-bonding network with the residues of the hA_{2A} AR, similar to the one seen for the 7-amino derivatives, seemed to explain why compound **43**, among the 7-(alkyl/acyl)amino derivatives, is the only one that showed affinity at the hA_{2A} AR in the nanomolar range.

In conclusion, we have synthesized AR antagonists of the triazolotriazine class and use molecular modeling studies to explain the SAR. Among the most potent and selective novel compounds were a long-chain ether-containing amine congener **20** and its urethane-protected derivative **14**. Compound **20** and a 5-(aminomethyl)cyclohexylmethyl-amino derivative **31** were readily water-soluble up to 10 mM, thus

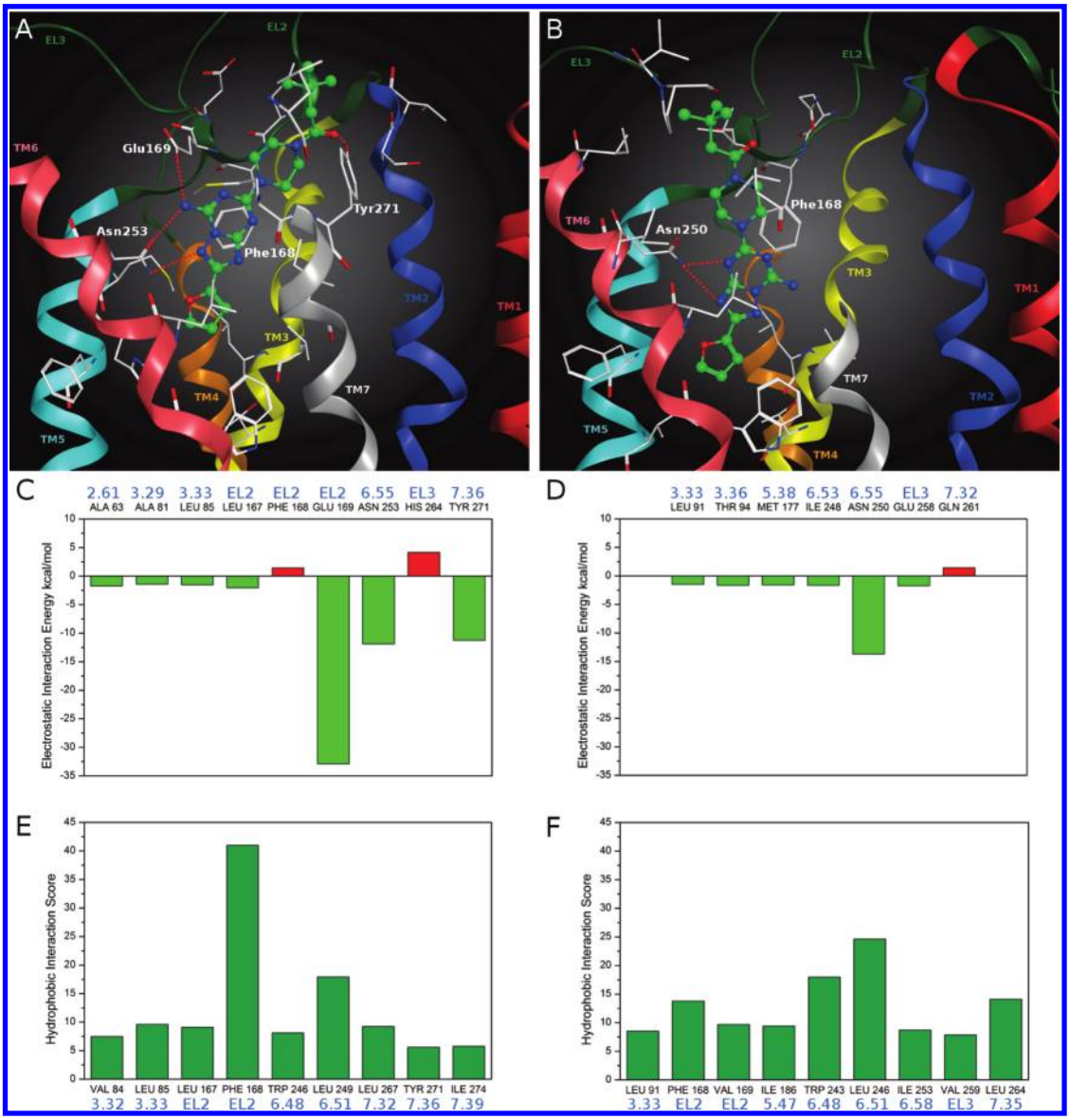

Figure 3. Hypothetical binding modes of compound **36** obtained after docking simulations: (A) inside the hA_{2A} AR binding site; (B) inside the hA_3 AR binding site. Poses are viewed from the membrane side facing TM6, TM7, and TM1. The view of TM7 is partially omitted. Side chains of some amino acids important for ligand recognition and H-bonding interactions are highlighted. Hydrogen atoms are not displayed. Electrostatic interaction energy (in kcal/mol) between the ligand and each single amino acid involved in ligand recognition observed from the hypothetical binding modes of compound **36** inside (C) hA_{2A} AR and (D) hA_3 AR binding sites. Hydrophobic interaction scores (in arbitrary hydrophobic units) between the ligand and each single amino acid involved in ligand recognition observed from the hypothetical binding modes of compound **36** inside (E) hA_{2A} AR and (F) hA_3 AR binding sites.

overcoming a common limitation of other bicyclic and tricyclic AR antagonists. *N*-Alkylated and *N*-acylated piperidine derivatives also displayed high affinity at the human A_{2A} AR, including an *N*-benzyl antagonist **19** and an *N*-3,3-dimethylbutanoyl derivative **36** that was roughly 900-fold selective versus both human A_1 and A_3 ARs. The analogues were docked in the crystallographic structure of hA_{2A} AR and in a homology model of the hA_3 AR, and the *per residue* electrostatic and hydrophobic contributions to the binding were assessed. The presence of a free amino group that seemed to be critical for the hA_{2A} affinity by allowing the ligands to participate in a H-bonding network with two critical residues of the binding site, Asn253 (6.55) and Glu169 (EL2). Another interaction found to be important for the hA_{2A} affinity of this series was the aromatic stacking between the triazole ring and Phe168 (EL2).

Conclusion

The present study has led to the identification of a new class of promising AR antagonists, the 1,2,4-triazolo[1,5-*a*]-1,3,5-triazine derivatives related to ZM241385. In particular, compound **20** (K_i 11.5 nM) and a 5-(aminomethyl)cyclohexylmethyl-amino derivative **31** (K_i 16.9 nM) were readily water-soluble up to 10 mM, thus overcoming a common limitation of other bicyclic and tricyclic AR antagonists. Finally, a receptor-based SAR has been proposed using a molecular modeling approach. All analogues were docked in the recently published crystallographic structure of hA_{2A} AR and in a homology model of the hA_3 AR, and the *per residue* electrostatic and hydrophobic contributions to the binding were assessed.

Molecular modeling results highlighted that all the newly synthesized 1,2,4-triazolo[1,5-*a*]-1,3,5-triazine derivatives with free amino group at the 7 position are characterized by a

common binding mode very similar to the crystallographic one of ZM241385 bound to the hA_{2A} AR. In fact, all the interactions found to be crucial for the X-ray structure, in particular the hydrogen bonding network with Asn253 (6.55), the Glu169 (EL2), and the aromatic stacking with Phe168 (EL2), were also important for anchoring these new derivatives to the hA_{2A} AR binding site. On the contrary, substitution at the 7 position was detrimental for the affinity at the hA_{2A} AR, as confirmed also by the orientation of the 7-(alkyl/acyl)amino derivatives inside the binding cavity that led to the loss of the stabilizing hydrogen bonding network.

Thus, we have probed points of substitution for attachment of solubilizing groups to enhance the aqueous solubility of this class of triazolotriazines, which are characterized by poor physicochemical properties. At the same time, potent interactions with the A_{2A} AR and, in some cases, receptor subtype selectivity have been maintained. We have used the A_{2A} AR X-ray structure to propose a structural basis for the activity and selectivity of this class of analogues and to direct the synthetic design strategy to provide access to solvent-exposed regions.

In general, the strategy of grafting a terminal polar tail on a pharmacophore, which increases the polar surface area, can have a detrimental effect on bioavailability and ion channel activity. Therefore, it will be necessary to evaluate these molecules in further pharmacological testing to see if they will be useful for in vivo studies.

Experimental Section

Chemical Synthesis. General. Reactions were routinely monitored by thin-layer chromatography (TLC) on silica gel (precoated F_{254} Merck plates). Infrared spectra (IR) were measured on a Jasco FT-IT instrument. ^{1}H NMR were determined in $CDCl_3$ or DMSO-d_6 solutions with a Varian Gemini 200 spectrometer, peaks positions are given in parts per million (δ) downfield from tetramethylsilane as internal standard, and J values are given in Hz. The following abbreviations were used: s, singlet; bs, broad singlet; d, doublet; dd, double doublet; t, triplet; m, multiplet.

Light petroleum ether refers to the fractions boiling at 40−60 °C. Melting points were determined on a Buchi-Tottoli instrument and are uncorrected. Flash chromatography was performed using Merck 60−200 mesh silica gel. Purity of compounds was detected by elemental analyses performed at the laboratory of microanalysis of the Department of Chemistry, University of Trieste (Italy), and all the compounds were confirmed to achieve 95% purity.

General Procedure for Nucleophilic Substitution with Amino Compounds (7, 8, 10−14). A mixture of compound **44** (0.29 g, 1 mmol) and the appropriate amine (**45**−**51**) (1.5 equiv) in absolute ethanol (5 mL) was poured into a sealed tube and heated at 120 °C for 3 h. Then the solvent was removed under reduced pressure and the residue crystallized from EtOAc-light petroleum to afford the desired compounds (**7**, **8**, **10**−**14**) as solids.

7-Amino-5-(*N*-pyrrolidinyl)-2(2-furyl) 1,2,4-triazolo [1,5-a] 1,3,5-triazine (8). Yield: 88%; brown solid (EtOAc-light petroleum) mp > 300 °C (dec.) ^{1}H NMR (DMSO-d_6) δ: 1.9−2.1 (m, 4H); 3.4−3.7 (m, 4H); 6.7 (dd, 1H, J = 2, J = 4); 7.1 (d, 1H, J = 2); 7.9 (d, 1H, J = 4); 8.4 (bs, 2H). IR (Nujol) cm^{-1}: 3350−3200, 1620, 1480. Anal. ($C_{12}H_{13}N_7O$) C, H, N.

7-Amino-5-[(4-*tert*-butyloxycarbonyl)-1-piperazinyl]-2(2-furyl) 1,2,4-triazolo [1,5-a] 1,3,5-triazine (7). Yield 73%; white solid (EtOAc-light petroleum) mp 250 °C. ^{1}H NMR (DMSO-d_6) δ: 1.4 (s, 9H); 3.4 (s, 4H); 3.8 (s, 4H); 6.7 (dd, 1H, J = 2, J = 4); 7.1 (d, 1H, J = 2); 7.9 (d, 1H, J = 4); 8.4 (bs, 2H). IR (Nujol) cm^{-1}: 3400−3150, 1735, 1630, 1510. Anal. ($C_{17}H_{22}N_8O_3$) C, H, N.

7-Amino-5-[(4-*tert*-butyloxycarbonylaminomethyl)cyclohexylmethyl]-amino-2(2-furyl) 1,2,4-triazolo [1,5-a] 1,3,5-triazine (11). Yield 76%; white solid (EtOAc-light petroleum) mp 148 °C. ^{1}H NMR ($CDCl_3$) δ: 1.2−2.0 (m, 6H); 1.4 (s, 9H); 2.9−3.2 (m, 2H); 3.3−3.5 (m, 2H); 4.6 (bs, 1H); 5.4 (bs, 1H); 6.7 (dd, 1H, J = 2, J = 4); 7.1 (d, 1H, J = 2); 7.3 (bs, 2H); 7.9 (bs, 2H). IR (Nujol) cm^{-1}: 3450−3100, 1735, 1620, 1470. Anal. ($C_{21}H_{28}N_8O_3$) C, H, N.

7-Amino-5-[(2-*tert*-butyloxycarbonylamino)ethyl]-amino-2(2-furyl) 1,2,4-triazolo [1,5-a] 1,3,5-triazine (10). Yield 63%; white solid (EtOAc-light petroleum) mp 168 °C. ^{1}H NMR (DMSO-d_6) δ: 1.4 (s, 9H); 3.1−3.4 (m, 4H); 6.7 (dd, 1H, J = 2, J = 4); 6.9 (bs, 1H); 7.1 (d, 1H, J = 2); 7.4 (bs, 1H); 7.9 (d, 1H, J = 4); 8.2 (bs, 2H). IR (Nujol) cm^{-1}: 3450−3150, 1740, 1630, 1500. Anal. ($C_{15}H_{20}N_8O_3$) C, H, N.

7-Amino-5-[(3-*tert*-butyloxycarbonylamino)propyl]-amino-2(2-furyl) 1,2,4-triazolo [1,5-a] 1,3,5-triazine (12). Yield 76%; white solid (EtOAc-light petroleum) mp 155 °C. ^{1}H NMR ($CDCl_3$) δ: 1.5 (s, 9H); 1.80−1.85 (m, 2H); 3.20−3.25 (m, 2H); 3.5−3.6 (m, 2H); 4.9 (bs, 1H); 5.4 (bs, 1H); 6.7 (dd, 1H, J = 2, J = 4); 7.1 (d, 1H, J = 2); 7.9 (d, 1H, J = 4); 7.9 (bs, 2H). IR (Nujol) cm^{-1}: 3400−3100, 1740, 1620, 1510. Anal. ($C_{16}H_{22}N_8O_3$) C, H, N.

7-Amino-5-[(5-*tert*-butyloxycarbonylamino)-*n*-pentyl]-amino-2(2-furyl) 1,2,4-triazolo [1,5-a] 1,3,5-triazine (13). Yield 71%; white solid (EtOAc-light petroleum) mp 140 °C. ^{1}H NMR ($CDCl_3$) δ: 1.4 (s, 9H); 1.6−1.8 (m, 6H); 3.2−3.3 (m, 2H); 3.50−3.55 (m, 2H); 4.7 (bs, 1H); 5.5 (bs, 1H); 6.40−6.43 (m, 2H); 6.7 (dd, 1H, J = 2, J = 4); 7.1 (d, 1H, J = 2); 7.9 (d, 1H, J = 4). IR (Nujol) cm^{-1}: 3450−3150, 1735, 1625, 1475. Anal. ($C_{18}H_{26}N_8O_3$) C, H, N.

7-Amino-5-[(8-*tert*-butyloxycarbonylamino)triethylenoxy]-amino-2(2-furyl) 1,2,4-triazolo [1,5-a] 1,3,5-triazine (14). Yield 64%; brown solid (EtOAc-light petroleum) mp 130 °C. ^{1}H NMR ($CDCl_3$) δ: 1.5 (s, 9H); 3.4−3.8 (m, 12H); 5.5 (bs, 1H); 6.2 (bs, 1H); 6.7 (dd, 1H, J = 2, J = 4); 7.1 (d, 1H, J = 2); 7.9 (d, 1H, J = 4); 9.4 (bs, 2H). IR (Nujol) cm^{-1}: 3400−3100, 1740, 1610, 1450. Anal. ($C_{19}H_{28}N_8O_5$) C, H, N.

Procedure for Preparation of 5,7-*bis*-[(2-*tert*-butyloxycarbonylamino) ethyl]-amino-2-(2-furyl)-1,2,4-triazolo [1,5-a] 1,3, 5-triazine (37). A mixture of compound **44** (0.29 g, 1 mmol) and the mono Boc ethylendiamine (**47**) (0.8 g, 5 equiv) in absolute ethanol (5 mL) was poured into a sealed tube and heated at 180 °C for 8 h. Then the solvent was removed under reduced pressure and the residue was crystallized from EtOAc-light petroleum to afford the desired compound (**37**) as a white solid in a good yield (70%). mp 154 °C. ^{1}H NMR (DMSO-d_6) δ: 1.4 (s, 18H); 3.0−3.4 (m, 8H); 6.7 (dd, 1H, J = 2, J = 4); 6.9 (bs, 1H); 7.1 (d, 1H, J = 2);7.6 (bs, 1H); 7.9 (d, 1H, J = 4); 8.5 (bs, 1H); 8.7 (bs, 1H). IR (Nujol) cm^{-1}: 3450, 1730, 1610, 1450. Anal. ($C_{22}H_{33}N_9O_5$) C, H, N.

General Procedure for *N*-Boc Deprotection (9, 20, 30−33, 38). Ten millimoles of the appropriate *N*-Boc derivative (**7**, **8**, **10**−**14**, **37**) was suspended in a 10% solution of CF_3COOH in dry CH_2Cl_2 and stirred at room temperature for 3 h. Then the solvent was removed under reduced pressure and the residue was crystallized from AcOEt-light petroleum to give the desired trifluoroacetate salts (**9**, **20**, **30**−**33**, **38**) as solids.

5,7-Bis-(amino)ethyl-amino-2(2-furyl) 1,2,4-triazolo [1,5-a] 1, 3,5-triazine *bis*-trifluoroacetate (38). Yield 63%; brown solid (EtOAc-light petroleum) mp 203 °C. ^{1}H NMR (DMSO-d_6) δ: 3.4−3.6 (m, 8H); 6.7 (dd, 1H, J = 2, J = 4); 7.1 (d, 1H, J = 2); 7.9 (d, 1H, J = 4); 8.0 (bs, 1H); 8.0 (bs, 3H). IR (Nujol) cm^{-1}: 3500−3100, 1630, 1500. Anal. ($C_{16}H_{19}N_9O_5F_6$) C, H, N.

7-Amino-5-(1-piperazinyl)-2(2-furyl) 1,2,4-triazolo [1,5-a] 1,3, 5-triazine trifluoroacetate (9). Yield 58%; brown solid (EtOAc-light petroleum) mp 243 °C. ^{1}H NMR (DMSO-d_6) δ: 3.20−3.25 (m, 4H); 4.0−4.1 (m, 4H); 6.0 (bs, 2H); 6.7 (dd, 1H, J = 2, J = 4); 7.1 (d, 1H, J = 2); 7.9 (d, 1H, J = 4); 9.0 (bs, 2H). IR (Nujol) cm^{-1}: 3500−3000, 1630, 1510. Anal. ($C_{14}H_{15}N_8O_3F_3$) C, H, N.

7-Amino-5-(aminomethyl)cyclohexylmethyl-amino-2(2-furyl) 1, 2,4-triazolo [1,5-a] 1,3,5-triazine trifluoroacetate (31). Yield 66%; brown solid (EtOAc-light petroleum) mp 150 °C. ^{1}H NMR (DMSO-d_6) δ: 1.2−2.0 (m, 10H); 2.4−3.0 (m, 4H); 6.7 (dd, 1H,

$J = 2$, $J = 4$); 7.1 (d, 1H, $J = 2$); 7.9 (d, 1H, $J = 4$); 8.0 (bs, 2H). IR (Nujol) cm^{-1}: 3500−3050, 1640, 1500. Anal. ($C_{18}H_{23}N_8O_3F_3$) C, H, N.

7-Amino-5-(2-aminoethyl)-amino-2(2-furyl) 1,2,4-triazolo [1,5-a] 1,3,5-triazine trifluoroacetate (30). Yield 54%; brown solid (EtOAc-light petroleum) mp 243 °C. ^{1}H NMR (DMSO-d_6) δ: 3.4−3.6 (m, 4H); 6.7 (dd, 1H, $J = 2$, $J = 4$); 7.1 (d, 1H, $J = 2$); 7.5 (d, 1H, $J = 4$); 7.8 (bs, 2H); 8.4 (bs, 2H); 8.0 (bs, 3H). IR (Nujol) cm^{-1}: 3450−3150, 1630, 1510. Anal. ($C_{12}H_{13}N_8O_3F_3$) C, H, N.

7-Amino-5-(3-amino)propyl-amino-2(2-furyl) 1,2,4-triazolo [1,5-a] 1,3,5-triazine trifluoroacetate (32). Yield 69%; brown solid (EtOAc-light petroleum) mp 235 °C. ^{1}H NMR (DMSO-d_6) δ: 3.4−3.6 (m, 6H); 6.7 (dd, 1H, $J = 2$, $J = 4$); 7.1 (d, 1H, $J = 2$); 7.5 (d, 1H, $J = 4$); 7.8 (bs, 2H); 8.4 (bs, 2H); 8.0 (bs, 3H). IR (Nujol) cm^{-1}: 3470−3140, 1640, 1510. Anal. ($C_{13}H_{15}N_8O_3F_3$) C, H, N.

7-Amino-5-(5-amino)pentyl-amino-2(2-furyl) 1,2,4-triazolo [1,5-a] 1,3,5-triazine trifluoroacetate (33). Yield 71%; brown solid (EtOAc-light petroleum) mp 160 °C. ^{1}H NMR (DMSO-d_6) δ: 1.6−1.8 (m, 6H); 3.2 (m, 2H); 3.5 (m, 2H); 5.5 (bs, 1H); 6.4 (bd, 2H); 6.7 (dd, 1H, $J = 2$, $J = 4$); 7.1 (d, 1H, $J = 2$); 7.9 (d, 1H, $J = 4$); 8.0 (bs, 3H). IR (Nujol) cm^{-1}: 3480−3120, 1640, 1500. Anal. ($C_{15}H_{19}N_8O_3F_3$) C, H, N.

7-Amino-5-[(8-amino)triethylenoxy]-amino-2(2-furyl) 1,2,4-triazolo [1,5-a] 1,3,5-triazine trifluoroacetate (20). Yield 52%; brown solid (EtOAc-light petroleum) mp 243 °C. ^{1}H NMR (DMSO-d_6) δ: 3.4−3.8 (m, 12H); 5.5 (bs, 1H); 6.7 (dd, 1H, $J = 2$, $J = 4$); 7.1 (d, 1H, $J = 2$); 7.9 (d, 1H, $J = 4$); 9.4 (bs, 2H); 8.0 (bs, 3H). IR (Nujol) cm^{-1}: 3510−3150, 1630, 1510. Anal. ($C_{15}H_{22}N_8O_5F_3$) C, H, N.

General Procedure for *N*-Benzylation of a Piperazine Moiety (15−19). A mixture of compound **9** (0.2 g, 0.05 mmol) the appropriate benzyl halide (1.2 equiv), Et_3N (7.2 μL, 0.06 mmol) in dry dioxane (10 mL) was stirred at room temperature for 6 h. The solvent was removed in vacuo and the residue was dissolved in EtOAc (15 mL) and washed with water (3 × 5 mL). The organic phase was dried and solvent was removed under reduced pressure. The crude was purified by flash chromatography (EtOAc) to give the final compounds (**15−19**) as solids.

7-Amino-5-[(4-benzyl)-1-piperazinyl]-2(2-furyl) 1,2,4-triazolo [1,5-a] 1,3,5-triazine (15). Yield 63%; white solid (EtOAc-light petroleum) mp 242 °C. ^{1}H NMR (DMSO-d_6) δ: 2.5 (s, 4H); 3.6 (s, 2H); 3.9 (s, 4H); 6.2 (bs, 2H); 6.7 (dd, 1H, $J = 2$, $J = 4$); 7.1 (d, 1H, $J = 2$); 7.6 (d, 1H, $J = 4$); 7.1−7.4 (m, 5H). IR (Nujol) cm^{-1}: 3350−3100, 1610, 1470. Anal. ($C_{19}H_{20}N_8O$) C, H, N.

7-Amino-5-[(4-(3-chloro-benzyl)-1-piperazinyl]-2(2-furyl) 1,2,4-triazolo [1,5-a] 1,3,5-triazine (16). Yield 70%; white solid (EtOAc-light petroleum) mp 227 °C. ^{1}H NMR (DMSO d_6) δ: 2.5 (s, 4H); 3.5 (s, 2H); 3.8 (s, 4H); 6.7 (dd, 1H, $J = 2$, $J = 4$); 7.1 (d, 1H, $J = 2$); 7.3−7.5 (m, 4H); 7.9 (d, 1H, $J = 4$); 8.4 (bs, 2H). IR (Nujol) cm^{-1}: 3340−3100, 1620, 1480 Anal. ($C_{19}H_{19}N_8OCl$) C, H, N.

7-Amino-5-[(4-(4-fluoro-benzyl)-1-piperazinyl]-2(2-furyl) 1,2,4-triazolo [1,5-a] 1,3,5-triazine (17). Yield 66%; white solid (EtOAc-light petroleum) mp 260 °C. ^{1}H NMR (DMSO-d_6) δ: 2.5 (s, 4H); 3.5 (s, 2H); 3.8 (s, 4H); 6.7 (dd, 1H, $J = 2$, $J = 4$); 7.1 (d, 1H, $J = 2$); 7.1−7.4 (m, 4H); 7.9 (d, 1H, $J = 4$); 8.4 (bs, 2H). IR (Nujol) cm^{-1}: 3340−3110, 1630, 1480. Anal. ($C_{19}H_{19}N_8OF$) C, H, N.

7-Amino-5-[(4-(4-chloro-benzyl)-1-piperazinyl]-2(2-furyl) 1,2,4-triazolo [1,5-a] 1,3,5-triazine (18). Yield 73%; white solid (EtOAc-light petroleum) mp 274 °C. ^{1}H NMR (DMSO-d_6) δ: 2.5 (s, 4H); 3.5 (s, 2H); 3.8 (s, 4H); 6.7 (dd, 1H, $J = 2$, $J = 4$); 7.1 (d, 1H, $J = 2$); 7.3−7.5 (m, 4H); 7.9 (d, 1H, $J = 4$); 8.4 (bs, 2H). IR (Nujol) cm^{-1}: 3350−3110, 1620, 1470. Anal. ($C_{19}H_{19}N_8OCl$) C, H, N.

7-Amino-5-[(4-(4-bromo-benzyl)-1-piperazinyl]-2(2-furyl) 1,2,4-triazolo [1,5-a] 1,3,5-triazine (19). Yield 68%; white solid (EtOAc-light petroleum) mp 284 °C. ^{1}H NMR (DMSO-d_6) δ: 2.5 (s, 4H); 3.5 (s, 2H); 3.8 (s, 4H); 6.7 (dd, 1H, $J = 2$, $J = 4$); 7.1 (d, 1H, $J = 2$); 7.3 (d, 2H); 7.5 (d, 2H); 7.9 (d, 1H, $J = 4$); 8.4 (bs, 2H). IR (Nujol) cm^{-1}: 3340−3110, 1630, 1480. Anal. ($C_{19}H_{19}N_8OBr$) C, H, N.

General Procedure for *N*-Piperazine Acylation (21−29, 34−36). A mixture of compound **9** (0.2 g, 0.05 mmol) the appropriate acyl chloride (1.2 equiv), Et_3N (7.2 μL, 0.06 mmol) in dry dioxane (10 mL) was stirred at room temperature for 2 h. The solvent was removed in vacuo and the residue was dissolved in EtOAc (15 mL) and washed with water (3 × 5 mL). The organic phase was dried and solvent was removed under reduced pressure. The crude was purified by flash chromatography (EtOAc) to give the final compounds (**21−29**, **34−36**) as solids.

7-Amino-5-[(4-(pentanoyl))-1-piperazinyl]-2(2-furyl) 1,2,4-triazolo [1,5-a] 1,3,5-triazine (22). Yield 66%; yellow solid (EtOAc-light petroleum) mp 167 °C. ^{1}H NMR (DMSO-d_6) δ: 0.9 (t, 3H, $J = 7$); 3.0−3.2 (m, 10H); 3.5 (s, 2H); 3.8 (s, 2H); 6.7 (dd, 1H, $J = 2$, $J = 4$); 7.1 (d, 1H, $J = 2$); 7.9 (d, 1H, $J = 4$); 8.4 (bs, 2H). IR (Nujol) cm^{-1}: 3350−3100, 1685, 1620, 1500. Anal. ($C_{17}H_{22}N_8O_2$) C, H, N.

7-Amino-5-[(4-(benzoyl))-1-piperazinyl]-2(2-furyl) 1,2,4-triazolo [1,5-a] 1,3,5-triazine (27). Yield 69%; white solid (EtOAc-light petroleum) mp 290 °C. ^{1}H NMR (DMSO-d_6) δ: 3.4−3.9 (m, 8H); 6.7 (dd, 1H, $J = 2$, $J = 4$); 7.1 (d, 1H, $J = 2$); 7.5 (m, 5H); 7.9 (d, 1H, $J = 4$); 8.4 (bs, 2H). IR (Nujol) cm^{-1}: 3360−3120, 1670, 1620, 1510. Anal. ($C_{19}H_{18}N_8O_2$) C, H, N.

7-Amino-5-[(4-(benzyl-carbonyl))-1-piperazinyl]-2(2-furyl) 1,2,4-triazolo [1,5-a] 1,3,5-triazine (23). Yield 64%; pale brown solid (EtOAc-light petroleum) mp 240 °C. ^{1}H NMR (DMSO-d_6) δ: 3.5−3.7 (m, 8H); 3.8 (s, 2H); 6.7 (dd, 1H, $J = 2$, $J = 4$); 7.1 (d, 1H, $J = 2$); 7.2−7.4 (m, 5H); 7.9 (d, 1H, $J = 4$); 8.4 (bs, 2H). IR (Nujol) cm^{-1}: 3320−3100, 1680, 1610, 1500. Anal. ($C_{20}H_{20}N_8O_2$) C, H, N.

7-Amino-5-[(4-(2-bromo-benzyl-carbonyl))-1-piperazinyl]-2(2-furyl) 1,2,4-triazolo [1,5-a] 1,3,5-triazine (21). Yield 76%; white solid (EtOAc-light petroleum) mp 223 °C. ^{1}H NMR (DMSO-d_6) δ: 3.5−3.7 (m, 8H); 3.8 (s, 2H); 6.7 (dd, 1H, $J = 2$, $J = 4$); 7.1 (d, 1H, $J = 2$); 7.2−7.4 (m, 4H); 7.9 (d, 1H, $J = 4$); 8.4 (bs, 2H). IR (Nujol) cm^{-1}: 3315−3080, 1670, 1620, 1500. Anal. ($C_{20}H_{19}N_8O_2Br$) C, H, N.

7-Amino-5-[(4-(methoxycarbonylethylcarbonyl))-1-piperazinyl]-2(2-furyl) 1,2,4-triazolo [1,5-a] 1,3,5-triazine (24). Yield 74%; white solid (EtOAc-light petroleum) mp 160 °C. ^{1}H NMR (DMSO-d_6) δ: 2.3−2.7 (m, 4H); 3.3 (s, 3H); 3.7−3.9 (m, 8H); 6.7 (dd, 1H, $J = 2$, $J = 4$); 7.1 (d, 1H, $J = 2$); 7.9 (d, 1H, $J = 4$); 8.4 (bs, 2H). IR (Nujol) cm^{-1}: 3330−3110, 1665, 1615, 1510. Anal. ($C_{17}H_{20}N_8O_4$) C, H, N.

7-Amino-5-[(4-(dichloromethylcarbonyl))-1-piperazinyl]-2(2-furyl) 1,2,4-triazolo [1,5-a] 1,3,5-triazine (25). Yield 70%; white solid (EtOAc-light petroleum) mp 261 °C. ^{1}H NMR (DMSO-d_6) δ: 3.6 (s, 4H); 3.8 (s, 4H); 6.7 (dd, 1H, $J = 2$, $J = 4$); 7.0 (s, 1H); 7.1 (d, 1H, $J = 2$); 7.9 (d, 1H, $J = 4$); 8.4 (bs, 2H). IR (Nujol) cm^{-1}: 3320−3100, 1670, 1610, 1520. Anal. ($C_{14}H_{14}N_8O_2Cl_2$) C, H, N.

7-Amino-5-[(4-(4-nitrobenzoyl))-1-piperazinyl]-2(2-furyl) 1,2,4-triazolo [1,5-a] 1,3,5-triazine (26). Yield 69%; pale yellow solid (EtOAc-light petroleum) mp > 300 °C (dec) ^{1}H NMR (DMSO-d_6) δ: 3.7−3.9 (m, 8H); 6.7 (dd, 1H, $J = 2$, $J = 4$); 7.1 (d, 1H, $J = 2$); 7.7 (d, 2H); 7.9 (d, 1H, $J = 4$); 8.3 (d, 2H); 8.4 (bs, 2H). IR (Nujol) cm^{-1}: 3300−3110, 1665, 1615, 1510. Anal. ($C_{19}H_{17}N_9O_4$) C, H, N.

7-Amino-5-[(4-(4-chloro-benzyl-carbonyl))-1-piperazinyl]-2(2-furyl) 1,2,4-triazolo [1,5-a] 1,3,5-triazine (29). Yield 74%; white solid (EtOAc-light petroleum) mp 260 °C. ^{1}H NMR (DMSO-d_6) δ: 3.7−3.9 (m, 8H); 6.7 (dd, 1H, $J = 2$, $J = 4$); 7.1 (d, 1H, $J = 2$); 7.2 (d, 2H); 7.3 (d, 2H); 7.7 (d, 2H, $J = 9$); 7.9 (d, 1H, $J = 4$); 8.3 (d, 2H, $J = 9$); 8.4 (bs, 2H). IR (Nujol) cm^{-1}: 3300−3100, 1675, 1625, 1500. Anal. ($C_{20}H_{17}N_8O_2Cl$) C, H, N.

7-Amino-5-[(4-(3,3-dimethylbutanoyl))-1-piperazinyl]-2(2-furyl) 1,2,4-triazolo [1,5-a] 1,3,5-triazine (36). Yield 77%; white solid (EtOAc-light petroleum) mp 297 °C. ^{1}H NMR (DMSO-d_6) δ: 1.0 (s, 9H); 2.3 (s, 2H); 3.6 (s, 4H); 3.8 (s, 4H); 6.7 (dd, 1H, $J = 2$, $J = 4$); 7.1 (d, 1H, $J = 2$); 7.9 (d, 1H, $J = 4$); 8.4 (bs, 2H). IR (Nujol) cm^{-1}: 3290−3100, 1680, 1615, 1510. Anal. ($C_{18}H_{24}N_8O_2$) C, H, N.

7-Amino-5-[(4-(diphenylmethylcarbonyl))-1-piperazinyl]-2(2-furyl) 1,2,4-triazolo [1,5-a] 1,3,5-triazine (34). Yield 63%; white solid (EtOAc-light petroleum) mp 295 °C. ^{1}H NMR (DMSO-d_6) δ: 3.6 (s, 4H); 3.8 (s, 4H); 5.6 (s, 1H); 6.7 (dd, 1H, $J = 2$, $J = 4$); 7.1 (d, 1H, $J = 2$); 7.2−7.4 (m, 10H); 7.9 (d, 1H, $J = 4$); 8.4 (bs, 2H). IR (Nujol) cm^{-1}: 3310−3110, 1675, 1620, 1510. Anal. ($C_{26}H_{24}N_8O_2$) C, H, N.

7-Amino-5-[(4-(α-naphthoyl))-1-piperazinyl]-2(2-furyl) 1,2,4-triazolo [1,5-a] 1,3,5-triazine (28). Yield 69%; white solid (EtOAc-light petroleum) mp 305 °C. ^{1}H NMR (DMSO-d_6) δ: 3.6−4.0 (m, 8H); 6.7 (dd, 1H, J = 2, J = 4); 7.1 (d, 1H, J = 2); 7.5−8.1 (m, 7H); 7.9 (d, 1H, J = 4); 8.4 (bs, 2H). IR (Nujol) cm^{-1}: 3305−3100, 1670, 1610, 1500. Anal. ($C_{23}H_{20}N_8O_2$) C, H, N.

7-Amino-5-[(4-(*tert*-butylcarbonyl))-1-piperazinyl]-2(2-furyl) 1,2,4-triazolo [1,5-a] 1,3,5-triazine (35). Yield 74%; white solid (EtOAc-light petroleum) mp > 300 °C. ^{1}H NMR (DMSO-d_6) δ: 1.2 (s, 9H); 3.6−3.8 (m, 8H); 6.7 (dd, 1H, J = 2, J = 4); 7.1 (d, 1H, J = 2); 7.9 (d, 1H, J = 4); 8.4 (bs, 2H). IR (Nujol) cm^{-1}: 3300−3110, 1675, 1610, 1500. Anal. ($C_{17}H_{22}N_8O_2$) C, H, N.

Procedure for the Preparation of 5,7-Diamino-2(2-furyl) 1,2,4-triazolo [1,5-a] 1,3,5-triazine (41). A mixture of compound **44** (0.29 g, 1 mmol) in absolute ethanol saturated with gas ammonia (2 mL) was poured into a sealed tube and heated at 120 °C for 3 h. Then the solvent was removed under reduced pressure and the residue was crystallized from EtOAc-light petroleum to afford the desired compound (**41**) as a solid in a good yield (88%). White solid (EtOAc-light petroleum) mp > 300 °C. ^{1}H NMR (DMSO-d_6) δ: 6.68 (dd, 1H, J = 2, J = 4); 6.98 (bs, 2H); 7.13 (d, 1H, J = 2); 7.81 (d, 1H, J = 4); 8.03 (bs, 2H). IR (Nujol) cm^{-1}: 3300−3110, 1640, 1600, 1525. Anal. ($C_8H_7N_7O$) C, H, N.

Procedure for the Preparation of 7-Amino 5-hydroxy-2(2-furyl) 1,2,4-triazolo [1,5-a] 1,3,5-triazine (40). A mixture of compound **44** (0.29 g, 1 mmol) in 2 M KOH in absolute ethanol (2 mL) was poured into a sealed tube and heated at 120 °C for 3 h. Then the solvent was removed under reduced pressure and the residue was crystallized from EtOAc-light petroleum to afford the desired compound (**40**) as a solid in a good yield (76%). White solid (EtOAc-light petroleum) mp 206 °C. ^{1}H NMR (DMSO-d_6) δ: 6.65 (dd, 1H, J = 2, J = 4); 7.18 (d, 1H, J = 2); 7.93 (d, 1H, J = 4); 8.81 (bs, 2H); 12.13 (bs, 1H). IR (Nujol) cm^{-1}: 3350−3145, 1655, 1610, 1530. Anal. ($C_8H_6N_6O_2$) C, H, N.

General Procedure for the N7 Benzoylation (39, 42). A mixture of the appropriate amino compound compound (**40**, **44**) (0.1 mmol) benzoyl chloride (14 μL, 0.12 mmol), Et_3N (14 μL, 0.12 mmol) in dry dioxane (10 mL) was stirred at reflux for 12 h. The solvent was removed in vacuo and the residue was dissolved in EtOAc (15 mL) and washed with water (3 × 5 mL). The organic phase was dried and solvent was removed under reduced pressure. The crude was purified by flash chromatography (EtOAc) to give the final compounds (**39**, **42**) as solids.

5-Hydroxy-7-phenylcarbonylamino-2(2-furyl) 1,2,4-triazolo [1,5-a] 1,3,5-triazine (42). Yield 75%; white solid (EtOAc-light petroleum) mp 201 °C. ^{1}H NMR (DMSO-d_6) δ: 6.66 (dd, 1H, J = 2, J = 4); 7.21 (d, 1H, J = 2); 7.45−7.98 (m, 7H); 10.52 (bs, 1H). IR (Nujol) cm^{-1}: 3340−3150, 1687, 1635, 1615, 1530. Anal. ($C_{15}H_{10}N_6O_3$) C, H, N.

5-Phenoxy-7-phenylcarbonylamino-2(2-furyl) 1,2,4-triazolo [1,5-a] 1,3,5-triazine (39). Yield 87%; pale yellow solid (EtOAc-light petroleum) mp 229 °C (dec). ^{1}H NMR (DMSO-d_6) δ: 6.60 (dd, 1H, J = 2, J = 4); 7.12 (d, 1H, J = 2); 7.25−7.65 (m, 7H); 7.80−7.99 (m, 4H). IR (Nujol) cm^{-1}: 3325−3070, 1695, 1620, 1510. Anal. ($C_{21}H_{14}N_6O_3$) C, H, N.

Procedure for the Preparation of 5-amino-7-phenylcarbonylamino-2(2-furyl) 1,2,4-triazolo [1,5-a] 1,3,5-triazine trifluoroacetate (43). A mixture of compound **39** (0.39 g, 1 mmol) in absolute ethanol saturated with gas ammonia (3 mL) was poured into a sealed tube and heated at 120 °C for 3 h. Then the solvent was removed under reduced pressure and the residue was crystallized from EtOAc-light petroleum to afford the desired compound (**43**) as a solid in a good yield (70%). Pale brown solid (EtOAc-light petroleum) mp 187 °C. ^{1}H NMR (DMSO-d_6) δ: 6.62 (dd, 1H, J = 2, J = 4); 7.18 (d, 1H, J = 2); 7.38−7.52 (m, 3H); 7.60−7.81 (m, 4H); 7.99 (d, 1H, J = 4); 8.98 (bs, 1H). IR (Nujol) cm^{-1}: 3325−3105, 1690, 1640, 1605, 1540. Anal. ($C_{15}H_{11}N_7O_2$) C, H, N.

Biological Testing. Radioligand Binding to hA_1, A_{2A} and A_3 ARs. [^{3}H]DPCPX, [^{3}H]ZM241385, and [^{125}I]I-AB-MECA were utilized in radioligand binding assays to membranes prepared from HEK-293 cells expressing recombinant hA_1, and hA_3 ARs, and from CHO cells expressing the recombinant hA_{2A} AR, as previously described.[40−42] Adenosine deaminase (3 units/mL) was present during the preparation of the membranes, in a preincubation of 30 min at 30 °C, and during the incubation with the radioligands. All nonradioactive compounds were initially dissolved in DMSO and diluted with buffer to the final concentration, where the amount of DMSO never exceeded 2%. Incubations were terminated by rapid filtration over Whatman GF/B filters, using a Brandell cell harvester (Brandell, Gaithersburg, MD). The tubes were rinsed three times with 3 mL of buffer each. At least six different concentrations of competitor, spanning 3 orders of magnitude adjusted appropriately for the IC_{50} of each compound, were used. IC_{50} values, calculated with the nonlinear regression method implemented in GraphPad (Prism, San Diego, CA), were converted to K_i values as described.[47] Hill coefficients of the tested compounds were in the range of 0.8−1.1.

Adenylyl Cyclase Activity. Because of the lack of a suitable radioligand the affinity of antagonists and the relative potency of agonists at the A_{2B} AR was determined in adenylyl cyclase experiments. The procedure was carried out as described previously[43,44] with minor modifications. Membranes were incubated with about 150 000 cpm of [α-^{32}P]ATP for 20 min in the incubation mixture as described[43,44] without EGTA and NaCl. For agonists the EC_{50}-values for the stimulation of adenylyl cyclase were calculated with the Hill equation. Hill coefficients in all experiments were near unity. IC_{50} values for antagonist concentration-dependent inhibition of adenylyl cyclase stimulated by 5′-*N*-ethylcarboxamidoadenosine (NECA) were calculated accordingly.

Molecular Modeling. All modeling studies were carried out on a 20 CPU (Intel Core2 Quad CPU 2.40 GHz) Linux cluster. Homology modeling, energy calculation, and analyses of docking poses were performed using the Molecular Operating Environment (MOE, version 2009.10) suite.[48] The software package MOPAC (version 7),[49] implemented in MOE suite, was utilized for all quantum mechanical calculations. Docking simulations were performed using GOLD suite (version 1.3.2).[50]

Three-Dimensional Structures of hA_{2A} AR and hA_3 AR. The recently published crystallographic structure of hA_{2A} AR, in complex with the high affinity antagonist ZM241385 (PDB code: 3EML),[36] was used to perform the molecular docking studies at this receptor subtype.

Moreover, on the basis of the assumption that GPCRs share similar TM boundaries and overall topology, a homology model of the hA_3 AR was constructed with the software MOE, as previously reported,[37,38] using as template the crystal structure of hA_{2A} AR.[36]

The numbering of the amino acids follows the arbitrary scheme by Ballesteros and Weinstein. According to this scheme, each amino acid identifier starts with the helix number, followed by the position relative to a reference residue among the most conserved amino acid in that helix. The number 50 is arbitrarily assigned to the reference residue.[51]

Molecular Docking of hA_{2A} AR Antagonists. Ligand structures were built using MOE-builder tool, part of the MOE suite,[48] and were subjected to MMFF94x energy minimization until the rms conjugate gradient was < 0.05 kcal mol^{-1} Å^{-1}. Partial charges for the ligands were calculated using PM3/ESP methodology.

Four different programs have been used to calibrate our docking protocols: MOE-Dock,[48] GOLD,[50] Glide,[52] and PLANTS.[53] In particular, ZM241385 was redocked into the crystal structure of the hA_{2A} AR (PDB code: 3EML) with different docking algorithms and scoring functions, as already described.[37,39] Then, rmsd values between predicted and crystallographic positions of ZM241385 were calculated for each of the docking algorithms. The results showed that docking simulations performed with GOLD gave the lowest rmsd value, the

lowest mean rmsd value and the highest number of poses with rmsd value < 2.5 Å.

On the basis of the best docking performance, all antagonist structures were docked into the TM binding site of the hA_{2A} AR crystal structure and that of the hA_3 AR model by using the docking tool of the GOLD suite.[50] Searching was conducted within a user-specified docking sphere, using the Genetic Algorithm protocol and the GoldScore scoring function. GOLD performed a user-specified number of independent docking runs (25 in our specific case) and wrote the resulting conformations and their scores in a molecular database file. The resulting docked complexes (ligand and side chains of residues at 4.5 Å from the ligand) were subjected to MMFF94x energy minimization until the rms conjugate gradient was < 1 kcal mol^{-1} $Å^{-1}$. Partial charges for the ligands were calculated using MOPAC and PM3/ESP methodology.

Prediction of antagonist-receptor complex stability (in terms of corresponding pK_i value) and the quantitative analysis for nonbonded intermolecular interactions (H-bonds, transition metal, water bridges, hydrophobic, electrostatic) were calculated and visualized using several tools implemented in MOE suite.[48] Electrostatic and hydrophobic contributions to the binding energy of individual amino acids have been calculated using MOE.[48] To estimate the electrostatic contributions, atomic charges for the ligands were calculated using PM3/ESP methodology. Partial charges for protein amino acids were calculated on the basis of the AMBER99 force field.

Acknowledgment. The work coordinated by S.M. was carried out with financial support from the University of Padova, Italy, and the Italian Ministry for University and Research (MIUR), Rome, Italy. This research was also supported in part by the Intramural Research Program of the NIH, National Institute of Diabetes and Digestive and Kidney Diseases. S.M. is very grateful to Chemical Computing Group Inc. (Montreal, Quebec, Canada) for the scientific and technical partnership.

Supporting Information Available: Elemental analyses and modeling figures. This material is available free of charge via the Internet at http://pubs.acs.org.

References

(1) Fredholm, B. B.; Arslan, G.; Halldner, L.; Kull, B.; Schulte, G.; Wasserman, W. Structure and function of adenosine receptors and their genes. *Naunyn-Schmiedeberg's Arch. Pharmacol.* **2000**, *362*, 364–374.

(2) Downey, J. M.; Cohen, M. V.; Ytrehus, K.; Liu, Y. Cellular mechanisms in ischemic preconditioning: the role of adenosine and protein kinase Ca. *Ann. N.Y. Acad. Sci.* **1994**, *723*, 82–98.

(3) Auchampach, J. A.; Jin, X.; Wan, T. C.; Caughey, G. H.; Linden., J. Canine mast cell adenosine receptors: cloning and expression of the A_3 receptor and evidence that degranulation is mediated by the A_{2B} receptor. *Mol. Pharmacol.* **1997**, *52*, 846–860.

(4) Jacobson, K. A.; von Lubitz, D. K. J. E.; Daly, J. W.; Fredholm, B. B. Adenosine receptor ligands: differences with acute versus chronic treatment. *Trends Pharmacol. Sci.* **1996**, *17*, 108–113.

(5) Fredholm, B. B. Adenosine and neuroprotection. *Int. Rev. Neurobiol.* **1997**, *40*, 259–280.

(6) Feoktistov, I.; Polosa, R.; Holgate, S. T.; Biaggioni, I. Adenosine A_{2B} receptors: a novel therapeutic target in asthma? *Trends Pharmacol. Sci.* **1998**, *19*, 148–153.

(7) Fozard, J. R.; McCarthy, C. Adenosine receptor ligands as potential therapeutics in asthma. *Curr. Opin. Invest. Drugs* **2002**, *3*, 69–77.

(8) Richardson, P. J.; Kase, H.; Jenner, P. G. Adenosine A_{2A} receptor antagonists as new agents for the treatment of Parkinson's disease. *Trends Pharmacol. Sci.* **1997**, *18*, 338–344.

(9) Ribeiro, J. A.; Sebastiao, A. M.; de Mendonca, A. Adenosine receptors in the nervous system: pathophysiological implications. *Prog. Neurobiol.* **2002**, *68*, 377–392.

(10) Yan, L.; Burbiel, J. C.; Maass, A.; Müller, C. E. Adenosine receptor agonists: from basic medicinal chemistry to clinical development. *Expert Opin. Emerg. Drugs* **2003**, *8*, 537–576.

(11) Fredholm, B. B. Adenosine receptors as targets for drug development. *Drug News Perspect.* **2003**, *16*, 283–289.

(12) Moro, S.; Spalluto, G.; Jacobson, K. A. Techniques: Recent developments in computer-aided engineering of GPCR ligands using the human A_3 adenosine receptor as an example. *Trends Pharmacol. Sci.* **2005**, *26*, 44–51.

(13) (a) Fredholm, B. B.; IJzerman, A. P.; Jacobson, K. A.; Klotz, K. N.; Linden, J. International Union of Pharmacology. XXV. Nomenclature and classification of adenosine receptors. *Pharmacol. Rev.* **2001**, *53*, 527–552. (b) Moro, S.; Gao, Z. G.; Jacobson, K. A.; Spalluto, G. Progress in the pursuit of therapeutic adenosine receptor antagonists. *Med. Res. Rev.* **2006**, *26*, 131–159.

(14) Baraldi, P. G.; Cacciari, B.; Romagnoli, R.; Spalluto, G.; Monopoli, A.; Ongini, E.; Varani, K.; Borea, P. A. 7-Substituted 5-amino-2-(2-furyl)pyrazolo[4,3-e]-1,2,4-triazolo[1,5-c]pyrimidines as A_{2A} adenosine receptor antagonists: a study on the importance of modifications at the side chain on the activity and solubility. *J. Med. Chem.* **2002**, *45*, 115–126.

(15) Baraldi, P. G.; Cacciari, B.; Spalluto, G.; Bergonzoni, M.; Dionisotti, S.; Ongini, E.; Varani, K.; Borea, P. A. Design, synthesis, and biological evaluation of a second generation of pyrazolo[4,3-e]-1,2,4-triazolo[1,5-c]pyrimidines as potent and selective A_{2A} adenosine receptor antagonists. *J. Med. Chem.* **1998**, *41*, 2126–2133.

(16) Baraldi, P. G.; Cacciari, B.; Spalluto, G.; Pineda de las Infantas y Villatoro, M. J.; Zocchi, C.; Dionisotti, S.; Ongini, E. Pyrazolo[4,3-e]-1,2,4-triazolo[1,5-c]pyrimidine derivatives: potent and selective A_{2A} adenosine antagonists. *J. Med. Chem.* **1996**, *39*, 1164–1171.

(17) Baraldi, P. G.; Cacciari, B.; Romagnoli, R.; Spalluto, G.; Klotz, K.-N.; Leung, E.; Varani, K.; Gessi, S.; Merighi, S.; Borea, P. A. Pyrazolo[4,3-e]1,2,4-triazolo[1,5-c]pyrimidine derivatives as highly potent and selective human A_3 adenosine receptor antagonists. *J. Med. Chem.* **1999**, *42*, 4473–4478.

(18) Baraldi, P. G.; Cacciari, B.; Romagnoli, R.; Spalluto, G.; Moro, S.; Klotz, K. N.; Leung, E.; Varani, K.; Gessi, S.; Merighi, S.; Borea, P. A. Pyrazolo[4,3-e]1,2,4-triazolo[1,5-c]pyrimidine derivatives as highly potent and selective human A_3 adenosine receptor antagonists: Influence of the chain at N^8 pyrazole nitrogen. *J. Med. Chem.* **2000**, *43*, 4768–4780.

(19) Baraldi, P. G.; Cacciari, B.; Moro, S.; Spalluto, G.; Pastorin, G.; Da Ros, T.; Klotz, K.-N.; Varani, K.; Gessi, S.; Borea, P. A. Synthesis, biological activity, and molecular modeling investigation of new pyrazolo[4,3-e]1,2,4-triazolo[1,5-c]pyrimidine derivatives as human A_3 adenosine receptor antagonists. *J. Med. Chem.* **2002**, *45*, 770–780.

(20) Maconi, A.; Pastorin, G.; Da Ros, T.; Spalluto, G.; Gao, Z. G.; Jacobson, K. A.; Baraldi, P. G.; Cacciari, B.; Varani, K.; Borea, P. A. Synthesis, biological properties and molecular modeling investigation of the first potent, selective and water soluble human A_3 adenosine receptor antagonist. *J. Med. Chem.* **2002**, *45*, 3579–3582.

(21) Pastorin, G.; Da Ros, T.; Spalluto, G.; Deflorian, F.; Moro, S.; Cacciari, B.; Baraldi, P. G.; Gessi, S.; Varani, K.; Borea, P. A. Pyrazolo[4,3-e]-1,2,4-triazolo[1,5-c]pyrimidine derivatives as adenosine receptor antagonists. Influence of the N5 substituent on the affinity at the human A_3 and A_{2B} adenosine receptor subtypes: a molecular modeling investigation. *J. Med. Chem.* **2003**, *46*, 4287–96.

(22) Cheong, S. L.; Dolzhenko, A.; Kachler, S.; Paoletta, S.; Federico, S.; Cacciari, B.; Dolzhenko, A.; Klotz, K. N.; Moro, S.; Spalluto, G.; Pastorin, G. The significance of 2-furyl substitutions with a 2-(para-substituted) aryl group in a new series of pyrazolo-triazolo-pyrimidines as potent and highly selective hA_3 adenosine receptor antagonists: new insight into structure activity relationship and receptor antagonist recognition. *J. Med. Chem.* **2010**, *53*, 3361–3375.

(23) Pinna, A.; Volpini, R.; Cristalli, G.; Morelli, M. New adenosine A_{2A} receptor antagonists: actions on Parkinson's disease models. *Eur. J. Pharmacol.* **2005**, *512*, 157–164.

(24) Vu, C. B.; Pan, D.; Peng, B.; Kumaravel, G.; Phadke, D.; Engber, T.; Huamg, C.; Reilly, J.; Tam, S.; Petter, R. C. Studies on adenosine A_{2A} receptor antagonists: comparison of three core heterocycles. *Bioorg. Med. Chem. Lett.* **2004**, *14*, 4831–4834.

(25) Dowling, J. E.; Vessels, J. T.; Haque, S.; Chang, H. X.; van Vloten, K.; Kumaravel, G.; Engber, T. M.; Jin, X.; Phadke, D.; Wang, J.; Ayyub, E.; Petter, R. C. Synthesis of [1,2,4]triazolo[1,5-a]pyrazines as adenosine A_{2A} receptor antagonists. *Bioorg. Med. Chem. Lett.* **2005**, *15*, 4809–4813.

(26) Gang, Y.; Haque, S.; Sha, L.; Kumaravel, G.; Wang, J.; Engber, T. M.; Whalley, E. T.; Conlon, P. R.; Chang, H.; Kiesman, W. F.; Petter, R. C. Synthesis of alkyne derivatives of novel triazolopyrazines as A_{2A} adenosine receptor antagonists. *Bioorg. Med. Chem. Lett.* **2005**, *15*, 511–515.

(27) Vu, C. B.; Shields, P.; Peng, B.; Kumaravel, G.; Jin, X.; Phadke, D.; Wang, J.; Engber, T.; Ayyub, E.; Petter, R. C. Triamino derivatives of triazolo triazine and triazolopyrimidines as adenosine A_{2A} receptor antagonists. *Bioorg. Med. Chem. Lett.* **2004**, *14*, 4835–4838.
(28) Peng, B.; Kumaravel, G.; Yao, G.; Sha, L.; Van Vlijmen, H.; Bohnert, T.; Huang, C.; Vu, C. B.; Ensinger, C. L.; Chang, H.; Engber, T. M.; Whalley, E.; Petter, R. C. Novel bicyclic piperazine derivatives of triazolotriazine and triazolopyrimidine as highly potent and selective adenosine A_{2A} receptor antagonists. *J. Med. Chem.* **2004**, *47*, 6218–6229.
(29) Vu, C. B.; Pan, D.; Kumaravel, G.; Smits, G.; Jin, X.; Phadke, D.; Engber, T.; Huang, C.; Reilly, J.; Tam, S.; Grant, D.; Hetu, G.; Petter, R. C. Novel diamino derivatives of [1,2,4]triazolo[1,5-a] [1,3,5]triazine as potent and selective adenosine A_{2A} receptor antagonists. *J. Med. Chem.* **2005**, *48*, 2009–2018.
(30) Poucher, S. M.; Keddie, J. R.; Singh, P.; Stoggall, S. M.; Caulkett, P. W. R.; Jones, G.; Collis, M. G. The in vitro pharmacology of ZM 241385, a potent, non-xanthine A2a selective adenosine receptor antagonist. *Br. J. Pharmacol.* **1995**, *115*, 1096–1102.
(31) DeZwart, M.; Vollinga, R. C.; Beukers, M. W.; Sleegers, D. F.; von Frijtag Drabbe Kunzel, J. K.; De Groote, M.; IJzerman, A. P. Potent antagonists for the human adenosine A_{2B} receptor. Derivatives of the triazolotriazine adenosine receptor antagonist ZM241385 with high affinity. *Drug Dev. Res.* **1999**, *48*, 95–103.
(32) Ji, X. D.; Jacobson, K. A. Use of triazolotriazine [^{3}H]-ZM241385 as a radioligand at recombinant human A_{2B} adenosine receptors. *Drug Des. Discovery* **1999**, *16*, 217–226.
(33) Pastorin, G.; Federico, S.; Paoletta, S.; Corradino, M.; Cateni, F.; Cacciari, B.; Klotz, K. N.; Gao, Z. G.; Jacobson, K. A.; Spalluto, G.; Moro, S. Synthesis and pharmacological characterization of a new series of 5,7-disubstituted [1,2,4]triazolo[1,5-a] [1,3,5]triazine derivatives as adenosine receptor antagonists: a preliminary inspection of ligand-receptor recognition process. *Bioorg. Med. Chem.* **2010**, *18*, 2524–2536.
(34) Caulkett, P. W. R.; Jones, G.; McPartlin, M.; Renshaw, N. D.; Stewart, S. K.; Wright., B. Adenine isosteres with bridgehead nitrogen. Part 1. Two independent syntheses of the [1,2,4]triazolo-[1,5-a][1,3,5]triazine ring system leading to a range of substituents in the 2, 5 and 7 positions. *J. Chem. Soc. Perkin Trans. I* **1995**, 801–808.
(35) Lee, D. W.; Ha, H. J.; Lee, W. K. Selective mono Boc-protection of diamines. *Synth. Commun.* **2007**, *37*, 737–742.
(36) Jaakola, V. P.; Griffith, M. T.; Hanson, M. A.; Cherezov, V.; Chien, E. Y. T.; Lane, J. R.; IJzerman, A. P.; Stevens, R. C. The 2.6 angstrom crystal structure of a human A_{2A} adenosine receptor bound to an antagonist. *Science* **2008**, *322*, 1211–1217.
(37) Lenzi, O.; Colotta, V.; Catarzi, D.; Varano, F.; Poli, D.; Filacchioni, G.; Varani, K.; Vincenzi, F.; Borea, P. A.; Paoletta, S.; Morizzo, E.; Moro, S. 2-Phenylpyrazolo[4,3-d]pyrimidin-7-one as a new scaffold to obtain potent and selective human A_3 adenosine receptor antagonists: new insights into the receptor-antagonist recognition. *J. Med. Chem.* **2009**, *52*, 7640–7652.
(38) Morizzo, E.; Federico, S.; Spalluto, G.; Moro, S. Human A_3 adenosine receptor as versatile G protein-coupled receptor example to validate the receptor homology modeling technology. *Curr. Pharm. Des.* **2009**, *15*, 4069–4084.
(39) Pastorin, G.; Federico, S.; Paoletta, S.; Corradino, M.; Cateni, F.; Cacciari, B.; Klotz, K.-N.; Gao, Z.-G.; Jacobson, K. A.; Spalluto, G.; Moro, S. Synthesis and pharmacological characterization of a new series of 5,7-disubstituted-[1,2,4]triazolo[1,5-a][1,3,5]triazine derivatives as adenosine receptor antagonists: A preliminary inspection of ligand-receptor recognition process. *Bioorg. Med. Chem.* **2010**, *18* (7), 2524–2536.
(40) Bruns, R. F.; Fergus, J. H.; Badger, E. W.; Bristol, J. A.; Santay, L. A.; Hartman, J. D.; Hays, S. J.; Huang, C. C. Binding of the A_1-selective adenosine antagonist 8-cyclopentyl-1,3-dipropylxanthine to rat brain membranes. *Naunyn-Schmiedeberg's Arch. Pharmacol.* **1987**, *335*, 59–63.
(41) Palmer, T. M.; Poucher, S. M.; Jacobson, K. A.; Stiles, G. L. ^{125}I-4-(2-[7-Amino-2-{furyl}{1,2,4}triazolo{2,3-a}{1,3,5}triazin-5-ylaminoethyl)phenol (^{125}I-ZM241385), a high affinity antagonist radioligand selective for the A_{2a} adenosine receptor. *Mol. Pharmacol.* **1996**, *48*, 970–974.
(42) Olah, M. E.; Gallo-Rodriguez, C.; Jacobson, K. A.; Stiles, G. L. ^{125}I-4-Aminobenzyl-5′-N-methylcarboxamidoadenosine, a highaffinity radioligand for the rat A_3 adenosine receptor. *Mol. Pharmacol.* **1994**, *45*, 978–982.
(43) Klotz, K. N.; Hessling, J.; Hegler, J.; Owman, C.; Kull, B.; Fredholm, B. B.; Lohse, M. J. Comparative pharmacology of human adenosine receptor subtypes- characterization of stably transfected receptors in CHO cells. *Naunyn-Schmiedeberg's Arch. Pharmacol.* **1998**, *357*, 1–9.
(44) Klotz, K. N.; Cristalli, G.; Grifantini, M.; Vittori, S.; Lohse, M. J. Photoaffinity labeling of A_1-adenosine receptors. *J. Biol. Chem.* **1985**, *260* (14), 659–14664.
(45) Kim, J.; Wess, J.; van Rhee, M.; Schoneberg, T.; Jacobson, K. A. Site-directed mutagenesis identifies residues involved in ligand recognition in the human A_{2A} adenosine receptor. *J. Biol. Chem.* **1995**, *270*, 13987–13997.
(46) Kim, J.; Jiang, Q.; Glashofer, M.; Yehle, S.; Wess, J.; Jacobson, K. A. Glutamate residues in the second extracellular loop of the human A_{2a} adenosine receptor are required for ligand recognition. *Mol. Pharmacol.* **1996**, *49*, 683–691.
(47) Linden, J. Calculating the dissociation constant of an unlabeled compound from the concentration required to displace radiolabel binding by 50%. *J. Cyclic Nucleotide Res.* **1982**, *8*, 163–172.
(48) *MOE* (*Molecular Operating Environment*), version 2009.10; Chemical Computing Group Inc.: Montreal, Quebec, Canada, 2009; http://www.chemcomp.com.
(49) Stewart, J. J. P. *MOPAC 7*; Fujitsu Limited: Tokyo, Japan, 1993.
(50) *GOLD suite*, version 1.3.2; Cambridge Crystallographic Data Centre: Cambridge; http://www.ccdc.cam.ac.uk.
(51) Ballesteros, J. A.; Weinstein, H. Integrated methods for the construction of three dimensional models and computational probing of structure-function relationships in G-protein coupled receptors. *Methods Neurosci.* **1995**, *25*, 366–428.
(52) Halgren, T. A.; Myrphy, R. B.; Friesner, R. A.; Beard, H. S.; Frye, L. L.; Pollard, W. T. Glide: a new approach for rapid, accurate docking and scoring 1 methods and assessment of docking accuracy. *J. Med. Chem.* **2004**, *47*, 1739–1749.
(53) Korb, O.; Stützle, T.; Exner, T. E. Empirical Scoring Functions for advanced Protein-Ligand Docking with PLANTS. *J. Chem. Inf. Model* **2009**, *49*, 84–96.